Electronic Supplementary Information

Pyridyl-triazole ligands enable in situ generation of a highly active dihydride iridium(III) complex for formic acid dehydrogenation

Miriam Abán,[†] J. Marco Cuenca, Irene Embid, Alba de Toro, Pilar Gómez-Sal, Ernesto de Jesús, Marta Valencia* and Cristina G. Yebra*

Departamento de Química Orgánica y Química Inorgánica, Instituto de Investigación Química "Andrés M. del Río", Universidad de Alcalá, Campus Universitario, 28805 Alcalá de Henares (Madrid), Spain.

marta.valencia@uah.es, cgarcia.yebra@uah.es

Table of Contents

1. General

1.1. Synthetic Techniques

The synthesis of organic and organometallic compounds was performed under an argon atmosphere using Schlenk techniques. $[Cp^*IrCl_2]_2$,[1] and $[Cp^*Ir(CO)Cl_2]$[2] were prepared according to literature procedures. $[Cp^*Ir(CO)H_2]$ was prepared using a modified procedure to that described in the literature.[2] 2-Azido-5-(methyl)pyridine,[3] 2-azido-5-(trifluoromethyl)pyridine,[4] **La**,[5] and **Lb**[6] were prepared according to previously published methods. Solvents (HPLC grade) were either dried and distilled or purified by flash column chromatography and collected under argon, using a MBraun MB SPS solvent purification device. NEt_3 was dried with CaH_2 and distilled. Formic acid was degassed and kept under argon. All other reagents were purchased from commercial sources and used without further purification.

1.2. Instrumental Techniques

Catalysis. All catalytic reactions were conducted in a Man on the Moon gas release measurement kit, model X103. The experiments were carried out in a 20 mL reactor equipped with a pressure transducer.

NMR spectroscopy. NMR spectra were recorded using Varian Mercury 300, Bruker NEO 400, or Unity 500 Plus spectrometers. Chemical shifts (δ, parts per million) are referenced relative to $SiMe_4$ and measured by internal referencing to the ^{13}C and residual ^1H resonances of the deuterated solvents. Coupling constants (J) are reported in Hz.

Mass spectrometry. Mass spectra were recorded at the Analytical Services of the University of Alcalá using an Agilent 6210-TOF LC/MS mass spectrometer with an ESI ion source. Samples, dissolved in the appropriate solvent, were directly pumped into the mass spectrometer and analyzed without additives.

Elemental analyses. The C, H, and N analyses were performed by the Analytical Services of the University of Alcalá using a LECO CHNS-932 microanalyzer.

Gas Chromatography. The analysis of the gases generated during catalysis was performed in the Center for Applied Chemistry and Biotechnology (CQAB), at the University of Alcalá, using an Agilent 490 Micro GC (G3581A) gas chromatograph composed of three independent channels. Channel 1 is provided with a 10 m MolSieve 5Å column with a sensitivity of up to 1 ppm and optimized with an Agilent Technologies standard for refinery gas (H_2 and CO). Channel 2 is provided with a 10 m PPU

(PoraPLOT U) column allowing the detection of CO_2. Helium was used as a gas carrier. Gas samples were collected via syringe through the rubber septum.

1.3. Safety Statement

The procedures described in this report are detailed to ensure they can be safely reproduced by personnel trained in the common hazards of chemical synthesis (e.g., handling flammable solvents, cryogenic liquids, and using vacuum lines). All volatile substances should be handled in a fume hood. Glass containers with pressurized gases must be protected with a safety screen. The glassware used in this work may not be safe at pressures higher than those specified here. No unusual hazards are associated with the procedures described, provided they are carried out by trained personnel and at the scale reported.

2. Experimental Section

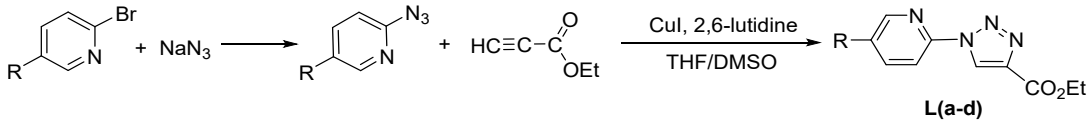

L(a-d)

a: R = H; **b**: R = CH_3O; **c**: R = CH_3; **d**: R = CF_3

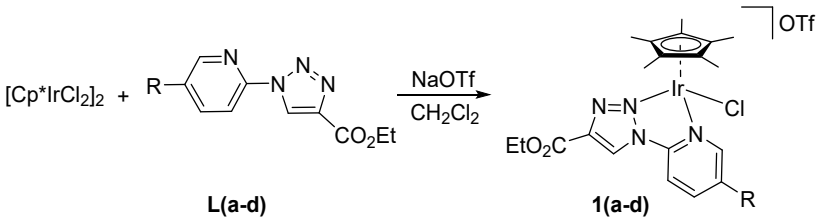

L(a-d) **1(a-d)**

a: R = H; **b**: R = CH_3O; **c**: R = CH_3; **d**: R = CF_3

2.1. Synthesis of Ligands Lc and Ld

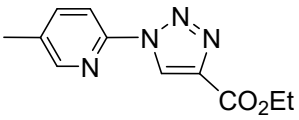

Synthesis of Lc. 2-Azido-5-(methyl)pyridine (200 mg, 1.48 mmol) was dissolved in THF/DMSO (7 mL, 99.3:0.7 v/v) in a 100 mL round bottom flask. Subsequently ethyl propionate (0.57 mL, 5.62 mmol), CuI (282 mg, 1.48 mmol) and 2,6-lutidine (345 µL, 2.96 mmol) were added. The mixture was stirred at 80 ˚C for 24 h. After cooling to room temperature, the mixture was washed with HCl 1M and brine, and the product extracted in ethyl acetate (2 x 5 mL). The organic layers were combined and dried over $MgSO_4$. After filtration, the solvent was evaporated to dryness and the remaining residue was purified by flash chromatography (SiO_2, hexane/ ethyl acetate 3:7). **Lc** was obtained as a light brown powder. Yield: (0.303 g, 88%). **^{1}H NMR (400 MHz, $CDCl_3$)**: δ 8.98 (s, 1H, CH_{trz}), 8.28 (s, 1H, CH_{py}), 8.05 (d, $^3J_{HH}$ = 8.2 Hz, 1H, CH_{py}), 7.70 (d, $^3J_{HH}$ = 8.2 Hz, 1H, CH_{py}), 4.41 (q, $^3J_{HH}$ = 7.1 Hz, 2H, CH_2CH_3), 2.38 (s, 3H, CH_3-pyr), 1.39 (t, $^3J_{HH}$ = 7.1 Hz, 3H, CH_2CH_3) ppm. **^{13}C{^{1}H} NMR (101 MHz, $CDCl_3$)**: δ 160.7 (s, CO), 148.8 (s, CH_{py}), 146.6 (s, C_{py}-trz), 140.4 (s, C_{trz}-CO), 139.8 (s, CH_{py}), 134.4 (s, C_{pyr}-CH_3), 124.6 (s, CH_{trz}), 113.6 (s, CH_{py}), 61.4 (s, CH_2CH_3), 18.1 (s, CH_3-pyr), 14.4 (s, CH_2CH_3) ppm. **Anal. Calcd. for $C_{11}H_{12}N_4O_2$** (232,243 g/mol): C, 56.89; H, 5.21; N, 24.12%. Found: C, 56.96; H, 5.40; N, 23.93%. **IR**: $\nu_{c=o}$ = 1735.1 cm^{-1}.

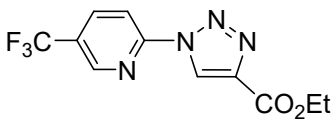

Synthesis of Ld. 2-Azido-5-(trifluoromethyl)pyridine (500 mg, 2.69 mmol) was dissolved in THF/DMSO (15.1

mL, 99.3:0.7 v/v) in a 50 mL round bottom flask covered with aluminium foil and under argon. Subsequently, ethyl propionate (0.82 mL, 8.06 mmol), CuI (512 mg, 2.69 mmol) and 2,6-lutidine (627 µL, 5.37 mmol) were added. The mixture was stirred at 80 ˚C for three days. After cooling to room temperature, the mixture was washed with HCl 1M and brine, and the product extracted with ethyl acetate (2 x 5 mL). The organic layers were combined and dried over $MgSO_4$. After filtration, the solvent evaporated under reduced pressure to give a residue that was purified by flash chromatography (SiO_2, hexane/ ethyl acetate 9:1). **Ld** was obtained as a white powder. Yield: 509.9 mg (67%). **^{1}H NMR (400 MHz, $CDCl_3$)**: δ 9.11 (s, 1H, CH_{trz}), 8.81 (m, 1H, CH_{py}), 8.40 (d, $^3J_{HH}$ = 8.6 Hz, 1H, CH_{py}), 8.21 (dd, $^3J_{HH}$ = 8.6, $^4J_{HH}$ = 2.3 Hz, 1H, CH_{py}), 4.47 (q, $^3J_{HH}$ = 7.2 Hz, 2H, CH_2CH_3), 1.44 (t, $^3J_{HH}$ = 7.2 Hz, 3H, CH_2CH_3) ppm. **^{13}C{^{1}H} NMR (126 MHz, $CDCl_3$)**: δ 160.4 (s, CO), 150.8 (s, Cpy-trz), 146.5 (q, $^3J_{CF}$ = 4.1 Hz, CH_{py}), 141.0 (s, C_{trz}-CO), 137.1 (q, $^3J_{CF}$ = 3.3 Hz, CH_{py}), 127.4 (q, $^2J_{CF}$ = 33.6 Hz, $C_{py\text{-}CF3}$), 125.2 (s, CH_{trz}), 123.0 (q, $^1J_{CF}$ = 272.4 Hz, CF_3), 114.2 (s, CH_{py}), 61.8 (s, CH_2CH_3), 14.4 (s, CH_2CH_3) ppm. ^{19}F NMR (282 MHz, $CDCl_3$): δ -63.11 (s, CF_3) ppm. **Anal. Calcd. for $C_{11}H_9F_3N_4O_2$** (286.2142 g/mol): C, 46.16; H, 3.17; N, 19.58%. Found: C, 46.18; H, 3.44; N, 19.48%. **IR**: $\nu_{c=o}$ = 1720.2 cm^{-1}.

2.2. Synthesis of Complexes 1a-d

General Procedure. In a 25 mL Schlenk flask under argon, one equivalent of $[Cp^*IrCl_2]_2$, two equivalents of the corresponding pyridyl-1,2,3-triazole ligand (**L**), and 2.1 equivalents of NaOTf were dissolved in 10 mL of dry dichloromethane. The reaction mixture was stirred at room temperature for 18 hours, then filtered through a pad of Celite. The filtrate was removed under reduced pressure. The remaining residue was washed with diethyl ether.

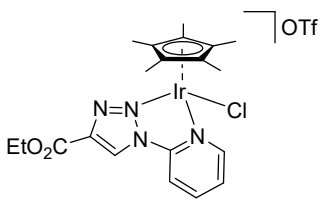

Synthesis of Complex 1a. La (109.5 mg, 0.502 mmol), $[Cp^*IrCl_2]_2$ (200 mg, 0.251 mmol), and NaOTf (90.7 mg, 0.527 mmol) were dissolved in dry CH_2Cl_2 (10 mL). **1a** was obtained as a yellow powder. Yield: 310.2 mg (85%). **HRMS** (ESI) m/z: 581.1284 calcd. for $C_{20}H_{25}ClIrN_4O_2$ [M^+], found 581.1249. **^{1}H NMR (500 MHz, $CDCl_3$):** δ 9.56 (s, 1H, CH_{trz}), 8.71 (d, $^3J_{HH}$ = 5.2 Hz, 1H, CH_{py}), 8.54 (d, $^3J_{HH}$ = 8.2 Hz, 1H, CH_{py}), 8.28 (dd, $^3J_{HH}$=8.2, 7.7 Hz, 1H, CH_{py}), 7.78 (dd, $^3J_{HH}$ = 6.3, 5.2 Hz, 1H, CH_{py}), 4.48 (q, $^3J_{HH}$ = 7.1 Hz, 2H, CH_2CH$_3$), 1.80 (s, 15H, CH_{3,Cp^*}), 1.43 (t, $^3J_{HH}$ = 7.1 Hz, 3H, CH$_2$CH_3) ppm. **^{13}C{^{1}H} NMR (126 MHz, $CDCl_3$):** δ 158.3 (s, *C*O), 150.4 (s, *C*H$_{py}$), 146.0 (s, C_{py}-trz), 143.5 (s, C_{trz}-CO), 143.3 (s, *C*H$_{py}$), 128.4 (s, *C*H$_{trz}$), 128.1 (s, *C*H$_{py}$), 120.7 (q, $^2J_{CF}$ = 320.3 Hz, $CF_3SO_3^-$), 115.9 (s, *C*H$_{py}$),

90.9 (s, C_{Cp*}), 62.7 (s, CH_2CH_3), 14.3 (s, CH_2CH_3), 8.9 (s, $CH_{3,Cp*}$) ppm. **^{19}F NMR (282 MHz, acetone-d_6)**: δ -78.86 (s, $CF_3SO_3^-$) ppm. **Anal. Calcd. for $C_{21}H_{25}ClF_3IrN_4O_5S$** (730.176 g/mol): C, 34.54; H, 3.45; N, 7.67; S, 4.39%. Found: C, 34.56; H, 3.48; N, 7.91; S, 4.21%. IR: $\nu_{c=o}$= 1735.1 cm^{-1}.

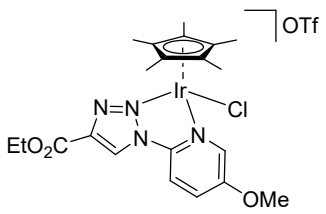

Synthesis of Complex 1b. Lb (93.8 mg, 0.376 mmol), $[Cp^*IrCl_2]_2$ (150 mg, 0.186 mmol), and NaOTf (68.1mg, 0.395 mmol) were dissolved in dry CH_2Cl_2 (10 mL). **1b** was obtained as a yellow powder. Yield: 205.5 mg (71%). **HRMS** (ESI) m/z: 611.1387 calcd for $C_{21}H_{27}ClIrN_4O_3$ [M$^+$], found 611.1384. **^{1}H NMR (500 MHz, $CDCl_3$):** δ 9.56 (s, 1H, CH_{trz}), 8.63 (d, $^3J_{HH}$ = 9.2 Hz, 1H, CH_{py}), 8.20 (d, $^4J_{HH}$ = 2.7 Hz, 1H, CH_{py}), 7.85 (dd, $^3J_{HH}$ = 9.2, $^4J_{HH}$ = 2.7 Hz, 1H, CH_{py}), 4.42 (q, $^3J_{HH}$ = 7.1 Hz, 2H, CH_2CH$_3$), 4.00 (s, 3H, OCH_3), 1.76 (s, 15H, C$H_{3,Cp*}$), 1.40 (t, $^3J_{HH}$ = 7.1 Hz, 3H, CH$_2$CH_3) ppm. **^{13}C{^{1}H} NMR (126 MHz, $CDCl_3$):** δ 158.4 (s, *C*O), 158.3 (s, $C_{py}OCH_3$), 143.3 (s, C_{trz}-CO), 139.2 (s, C_{py}-trz), 138.2 (s, *C*H$_{py}$), 127.6 (s, *C*H$_{trz}$), 126.1(s, *C*H$_{py}$), 120.5 (q, $^2J_{CF}$ = 320.3 Hz, $CF_3SO_3^-$), 116.7 (s, *C*H$_{py}$), 90.7 (s, C_{Cp*}), 62.4 (s, *C*H$_2$CH$_3$), 57.1 (s, O*C*H$_3$), 14.1 (s, CH$_2$*C*H$_3$), 8.8 (s, *C*H$_{3,Cp*}$) ppm. **Anal. Calcd. for $C_{22}H_{27}ClF_3IrN_4O_6S$** (760.2022 g/mol): C, 34.76; H, 3.58; N, 7.32, S 4.22%. Found: C, 34.36; H, 3.602; N 7.43; S, 4.32%. IR: $\nu_{c=o}$= 1750.0 cm^{-1}.

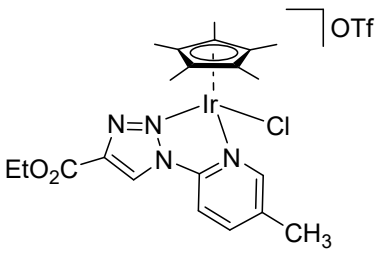

Synthesis of Complex 1c. Lc (58.3 mg, 0.251 mmol), $[Cp^*IrCl_2]_2$ (100 mg, 0.126 mmol), and NaOTf (45.3 mg, 0.263 mmol) were dissolved in dry CH_2Cl_2 (10 mL). After 18h, the reaction mixture was washed with water and extracted with CH_2Cl_2. The organic layer was dried with anhydrous $MgSO_4$ and the solvent was evaporated in vacuo. Then, the residue was washed with diethyl ether (3 x 2 mL). **1c** was obtained as a yellow powder. Yield: 144.4 mg (77%). **HRMS** (ESI) m/z: 595.1442 calcd for $C_{21}H_{27}ClIrN_4O_2$ [M$^+$], found 595.1407. **^{1}H NMR (500 MHz, $CDCl_3$):** δ 9.49 (s, 1H, CH_{trz}), 8.40 – 8.34 (m, 2H, CH_{py}), 8.12 (d, $^3J_{HH}$ = 8.2 Hz, 1H, CH_{py}), 4.47 (dq, $^2J_{HH}$ = 10.2, $^3J_{HH}$ = 7.1 Hz, 2H, CH_2CH$_3$), 2.57 (s, 3H, CH_3-py), 1.80 (s, 15H, C$H_{3,Cp*}$), 1.44 (dd, $^3J_{HH}$ = 7.1, 7.1 Hz, 3H, CH$_2$CH_3) ppm. **^{13}C{^{1}H} NMR (126 MHz, $CDCl_3$):** δ 158.3 (s, *C*O$_2$), 149.2 (s, *C*H$_{py}$), 144.2 (s, C_{pyr}-trz), 144.0 (s, *C*H$_{py}$), 143.4 (s, C_{trz}-CO), 138.6 (s, C_{pyr}-CH$_3$), 128.5 (s, *C*H$_{trz}$), 120.3 (q, $^2J_{CF}$ = 320.4 Hz, $CF_3SO_3^-$), 115.9 (s, *C*H$_{py}$), 90.7 (s, C_{Cp*}), 62.6 (s, CH_2CH$_3$), 18.7 (s, *C*H$_3$-pyr), 14.3 (s, CH$_2$*C*H$_3$), 9.0 (s, *C*H$_{3,Cp*}$) ppm. **^{19}F NMR (282 MHz, $CDCl_3$):** δ -79.22 (s, $CF_3SO_3^-$) ppm. **Anal. Calcd. for $C_{22}H_{27}ClF_3IrN_4O_5S$** (744.203 g/mol)·1$CH_2Cl_2$: C, 33.32; H, 3.53; N, 6.76; S, 3.87%; Found: C, 33.25; H, 3.61; N, 7.02; S, 3.57%. IR: $\nu_{c=o}$ = 1742.5 cm^{-1}.

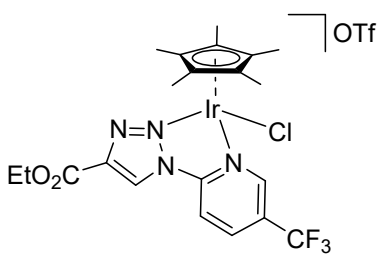

Synthesis of Complex 1d. Ld (78.1 mg, 0.251 mmol), $[Cp^*IrCl_2]_2$ (100 mg, 0.126 mmol), and NaOTf (43.2 mg, 0.251 mmol) were dissolved in dry CH_2Cl_2 (10 mL). After 18h, the reaction mixture was washed with water and extracted with CH_2Cl_2. The organic layer was dried with anhydrous $MgSO_4$ and the solvent was evaporated in vacuo. Then, the residue was washed with hexane (3 x 2 mL). **1d** was obtained as a yellow powder. Yield: 159.0mg (79%). **HRMS** (ESI) m/z: 649.1157 calcd for $C_{21}H_{24}ClF_3IrN_4O_2$ [M^+], found 649.1143. **^{1}H NMR (500 MHz, $CDCl_3$):** δ 9.77 (s, 1H, CH_{trz}), 8.91 (d, $^3J_{HH}$ = 8.7 Hz, 1H, CH_{py}), 8.76 (s, 1H, CH_{py}), 8.57 (dd, $^3J_{HH}$ = 8.7, $^3J_{HH}$ = 1.8 Hz, 1H, CH_{py}), 4.50 (q, $^3J_{HH}$ = 7.1 Hz, 2H, CH_2CH$_3$), 1.80 (s, 15H, CH_{3,Cp^*}), 1.42 (t, $^3J_{HH}$ = 7.1 Hz, 3H, CH_3CH$_2$) ppm. **^{13}C{^{1}H} NMR (126 MHz, $CDCl_3$):** δ 158.3 (s, CO$_2$), 148.7 (s, C_{py}-trz), 146.3 (s, CH$_{py}$), 143.6 (s, C_{trz}-CO), 140.5 (s, CH$_{py}$), 129.9 (q, $^2J_{CF}$ = 35.3 Hz, C_{pyr}-CF$_3$), 129.7 (s, CH$_{trz}$), 121.7 (q, $^1J_{CF}$ = 273.6, CF_3), 120.4 (q, $^2J_{CF}$ = 320.0 Hz. OTf) 117.3 (s, CH$_{py}$), 91.2 (s, C_{Cp^*}), 62.6 (s, CH$_2$CH$_3$), 14.2 (s, CH$_2$$CH_3$), 8.8 (s, CH$_{3,Cp^*}$) ppm. **^{19}F NMR (282 MHz, $CDCl_3$):** δ -63.19 (s, CF_3), -79.43 (s, CF_3O$_3$S) ppm. **Anal. Calcd. for $C_{22}H_{24}ClF_6IrN_4O_5S$** (798.174 g/mol): C, 33.11; H, 3.03; N, 7.02; S, 4.02%. Found: C, 32.91; H, 3.05; N, 7.27; S, 4.05%. IR: $\nu_{c=o}$ = 1742.5 cm^{-1}.

Stability of the complexes. Complexes **1a-1d** are indefinitely stable in the solid state and can be stored in air for years. In toluene solution, they remain stable at room temperature for months. No significant changes were observed when the solutions were heated up to 100˚C for hours.

2.3. Synthesis of Complex $[Cp^*Ir(CO)H_2]$ (2)

$[Cp^*Ir(CO)Cl_2]$ (50 mg, 0.11 mmol) and $NaBH_4$ (80 mg, 2.1 mmol) were dissolved in toluene (4 mL) under argon, inside a 50 mL Schlenk flask provided with a J. Young valve. After the dropwise addition of 0.3 mL of MeOH, the reaction was stirred for 18 h at room temperature and then filtered through Celite, using a canula. The solutions, which contained spectroscopically pure $[Cp^*Ir(CO)H_2]$, were used as is after titration (see below). $[Cp^*Ir(CO)H_2]$ (**2**) can be stored in solution under an H_2 atmosphere (2 bar) for months. Yield: 0.107 mmol (97%). Attempts to isolate $[Cp^*Ir(CO)H_2]$ as a solid result in its decomposition and formation of dimer $[Cp^*Ir(CO)]_2$.[2] However, the complex $[Cp^*Ir(CO)]_2$ can slowly undergo re-hydrogenation in solution over several months, ultimately leading to the recovery of $[Cp^*Ir(CO)H_2]$ (Section 6.3.1; Fig. S31).

^{1}H NMR (400 MHz, C_6D_6): δ 1.88 (s, 15H, CH_{3,Cp^*}), −15.75 (s, 2H, IrH$_2$).

^{1}H NMR (400 MHz, toluene-d_8): δ 1.91 (s, 15H, C$H_{3,Cp*}$), −15.91 (s, 2H, IrH_2).

Determination of the Molar Concentration of [Cp*Ir(CO)H_2] Solutions. The concentration of the toluene solutions of complex [Cp*Ir(CO)H_2] were determined by ^{1}H NMR. Three 50 μL samples of the solution were added to three separate NMR tubes. The solvent was then evaporated under an argon stream. Subsequently, C_6D_6 (0.5 mL) and mesitylene (0.3 μL, 2.09 μmol) were added as an internal standard. The average ratio of the integrals corresponding to the Cp* and mesitylene protons in the ^{1}H NMR spectra was used to calculate the concentration of the complex in the parent solution (Fig. S30).

2.4. General Procedure for the Dehydrogenation of Formic Acid (FA)

The experiments were carried out in a 20 mL reactor equipped with a pressure transducer (Man on the Moon gas release measurement kit, model X103). The reactor was loaded with the required amount of catalyst, solvent, and NEt_3 (if needed) under an argon atmosphere, and then heated to working temperature. Once a constant pressure reading was reached, the pressure transducer and stopwatch were set to zero. Either net formic acid (100 μL, 2.64 mmol) or a 10:1 formic acid/sodium formate mixture (91 μL mixture, 2.35 mmol HCOOH) was then injected through a septum. The relative reactor pressure was recorded at regular 15 s intervals thereafter. To avoid exceeding the reactor safety pressure, the relief valve was opened every time the absolute pressure inside the reactor exceeded approximately 2.5 bar.

The subsequent processing of these data with a spreadsheet allowed obtaining the TON and TOF values, which are a measure of the catalyst activity in terms of stability and process speed, respectively. The chemical amount of dihydrogen ($n(H_2)$) in moles was first calculated, considering an ideal gas behavior for the 1:1 mixture of gases CO_2 and H_2:

$$n(\text{gases}) = V\Delta P/(RT)$$
$$n(H_2) = n(\text{gases})/2$$

where ΔP is the cumulative pressure increase at the time of measurement, V the volume of the flask, R the ideal gas constant (0.082 atm L mol^{-1} K^{-1}), T the temperature of the system and $n(H_2)$ the moles of H_2 obtained.

The TON y TOF were calculated as follows:

$$\textbf{TON} = \frac{n(H_2)}{n_{cat}} \quad ; \qquad \textbf{TOF} = \text{TON} / \text{t}$$

where n_{cat} is the moles of catalyst used and t is the time elapsed from the addition of the formic acid to the time of measurement.

TOF is the TOF value at the end of the reaction (maximum conversion value).

TOF_{max} is the maximum value of TOF. The time corresponding to this maximum value is indicated in brackets on the tables.

TOF_{50} is the TOF value corresponding to 50 per cent conversion.

3. Tables

3.1. Dehydrogenation of Formic Acid in Toluene

Table S1. Optimization of Catalysis Conditions with Complex 1a.[a]

Entry	[1a] (mol%)	[NEt_3] (mol%)	Temp. (°C)	Reaction time (min)	TOF_{50} (h^{-1})	TOF (h^{-1})	TON
1	1	0	70	-	-	-	-
2	1	11	70	60	114	92	92
3	1	2.8	70	100	-	2	1
4	1	5.6	70	75	73	71	88
5	1	24	70	60	-	40	40
6	1	11	25	974	-	1	10
7	1	11	50	344	9	11	62
8	1	11	60	120	47	46	92
9	1	11	80	30	275	184	92
10	1	11	90	30	550	190	91
11	**0.5**	11	90	30	**733**	**299**	150

[a] HCOOH (10 µL, 0.264 mmol), NEt_3, complex **1a**, in toluene (1 mL).

Table S2. Catalytic FADH with Complexes 1a-1d.[a]

Entry	Catalyst (mol%)	Temp. (°C)	Reaction time (min)	TOF_{50} (h^{-1})	TON
1	**1a** (1)	70	60	114	92
2	**1b** (1)	70	60	72	84
3	**1c** (1)	70	60	89	90
4	**1d** (1)	70	60	158	91
5	**1a** (0.5)	90	30	733	150
6	**1b** (0.5)	90	30	717	154
7	**1c** (0.5)	90	30	635	142
8	**1d** (0.5)	90	30	760	159

[a] HCOOH (10 µL, 0.264 mmol), NEt_3 (4 µL, 11 mol%), complex **1** in toluene (1 mL).

Table S3. FADH Catalyzed by 1a at 70 °C.

Entry	Yield (%)	Reaction time (min)	TOF_{50} (h^{-1})	TOF (h^{-1})	TON
C1[a]	99	60	92	92	92
C2[b]	97	25	664	217	90
C3[b]	74	30	416	139	70
C4[b]	60	120	36	27	54

[a] Initial conditions: HCOOH (10 µL, 0.264 mmol), NEt_3 (4 µL, 11 mol%), complex **1a** (2.64×10^{-3} mmol, 1 mol%) in toluene (1 mL). [b] Subsequent addition of HCOOH (10 µL, 0.264 mmol) and NEt_3 (4 µL, 11 mol%).

3.2. Dehydrogenation of Neat Formic Acid

Table S4. Dehydrogenation of Neat HCOOH Catalyzed by Complexes 1a-1d Using NEt_3 as an Additive.[a]

Entry	Catalyst (mol%)	Reaction time (min)	TOF_{max} (h^{-1}) (time)	TOF_{50} (h^{-1})	TOF (h^{-1})	TON[b]
1	**1a** (0.1)	20	2215 (16 min)	1946	1862	680
2	**1b** (0.1)	40	1514 (26 min)	1192	1511	680
3	**1c** (0.1)	20	3301 (12 min)	2869	2161	720
4	**1d** (0.1)	20	3065 (14 min)	2465	2378	793
5	**1a** (0.01)	54	9332 (30 min)	9290	6400	5800

[a] HCOOH (100 µL, 2.64 mmol), NEt_3 (39 µL, 0.29 mmol, 11 mol%), **1a-d**, 100 °C. [b] Part of HCOOH condensed at the headspace of the reaction vessel, out of reach of the catalyst.

Table S5. Dehydrogenation of Neat Formic Acid by Complex 1d using NEt_3 as an additive: Recharges of HCOOH/NEt_3 without Catalyst Re-addition.

Entry	[1d] (mol%)	HCOOH (mmol)	[NEt_3] (mol%)	Reaction time (min)	TOF_{max} (h^{-1}) (time)	TOF_{50} (h^{-1})	TOF (h^{-1})	TON[c]
C1 [a]	0.1	2.64	11	20	3065 (14 min)	2465	2378	793
C2 [b]	--	2.64	11	40	2085 (16 min)	2045	1191	795
C3 [b]	--	2.64	11	40	2100 (17 min)	2037	1310	875
C4 [b]	--	2.64	11	60	1947 (16 min)	1946	839	839
C5 [b]	--	2.64	11	80	1237 (24 min)	1237	637	849
					Accumulated TON [d]			**4350**

[a] HCOOH (100 µL, 2.64 mmol), NEt_3 (39 µL, 0.29 mmol, 11 mol%), **1d** (2.1 mg; 2.63×10^{-3} mmol, 0.1 mol%), 100 °C. [b] Subsequent addition of HCOOH (100 µL, 2.64 mmol) and NEt_3 (39 µL, 0.29 mmol, 11 mol%). [c] Part of HCOOH condensed at the headspace of the reaction vessel, out of reach of the catalyst. [d] Accumulated TON over addition of 5 × 100 µL = 500 µL of HCOOH.

Table S6. Dehydrogenation of Neat Formic Acid by Complex 1d: Recharges of HCOOH without Catalyst Re-addition.[a]

Entry	[1d] (mol%)	HCOOH (mmol)	Temp. (˚C)	React time (min)	TOF_{max} (h^{-1}) (time)	TOF_{50} (h^{-1})	TOF (h^{-1})	TON [d]
C1 [b]	0.1	2.35	100	27	1749 (16min)	1699	1365	634
C2 [c]	--	2.64	100	28	4253 (9min)	3889	1787	862
C3 [c]	--	2.64	90	24	2598 (16min)	2347	2003	833
C4 [c]	--	2.64	90	52	2387 (17min)	2137	1017	892
C5 [c]	--	2.64	90	28	2395 (17min)	2144	1788	843
C6 [c]	--	2.64	90	35	2359 (19min)	2047	1521	912
C7 [c]	--	2.64	90	36	2078 (20min)	1891	1426	862
C8 [c]	--	2.64	90	21	2258 (15min)	2170	1879	674
C9 [c]	--	2.64	90	21	2287 (15min)	2173	1975	714
C10 [c]	--	2.64	90	22	1346 (19 min)		1268	476
							Accumulated TON [e]	**7702**

[a] The experiment requires the prior preparation of a 10:1 w/w mixture of formic acid / sodium formate. For this purpose, 360 mg (5.29 mmol) of HCOONa are dissolved in 2 mL (52.9 mmol, ρ = 1.2183 g/mL) of HCOOH. [b] A HCOOH/HCOONa solution (91 µL, 2.35 mmol of HCOOH) was added to **1d** (0.1 mol% Ir). [c] Subsequent addition of 100 µL (2.64 mmol) of neat HCOOH. [d] Part of HCOOH condensed at the headspace of the reaction vessel, out of reach of the catalyst. [e] Accumulated TON over addition of HCOOH (~ 10 x 100 µL = 1 mL).

Table S7. Dehydrogenation of Neat Formic Acid by Complex 1d: Recharges of HCOOH without Catalyst Re-addition[a]

Entry	[1d] (mol%)	HCOOH (mmol)	Reaction time (min)	TOF_{max} (h^{-1}) (time)	TOF_{50} (h^{-1})	TOF (h^{-1})	TON[d]
1-C1 [b]	0.02	2.35[a]	31	5208 (30 min)	5179	5135	2693
1-C2 [c]	-	2.64	36	9855 (27 min)	8395	8249	5026
1-C3 [c]	-	2.64	47	7492 (35 min)	6329	6239	4911
1-C4 [c]	-	2.64	44	8237 (33 min)	4098	6880	5139
1-C5 [c]	-	2.64	39	8263 (33 min)	7080	7551	4968
1-C6 [c]	-	2.64	44	8072 (33 min)	6982	6894	5139
					Accumulated TON[e]		26876
2-C1 [b]	0.01	2.35[a]	42	8921 (37 min)	8251	8385	5902
2-C2 [c]	-	2.64	46	10703 (46 min)	8942	10703	8232
					Accumulated TON[e]		14134

[a] The experiment requires the prior preparation of a 10:1 mixture of formic acid (M = 46.03 g/mol; ρ = 1.2183 g/mL) / sodium formate (M = 68.01 g/mol). For this purpose, 360 mg (5.29 mmol) of HCOONa is dissolved in 2 mL (52.9 mmol) of HCOOH. [b] A HCOOH / HCOONa solution (91 µL, 2.35 mmol of HCOOH) was added to **1d** at 90 ˚C. [c] Subsequent addition of 100 µL (2.64 mmol) of neat HCOOH at 90 ˚C. [d] Part of HCOOH condensed at the headspace of the reaction vessel, out of reach of the catalyst. [e] Accumulated TON over addition of HCOOH.

3.3. Kinetic Isotopic Effect.

Table S8. Kinetic Isotopic Effect (KIE) Data [a]

Entry	Formic acid / sodium formate	TOF_{max} (h^{-1})	KIE	
1	HCOOH / HCOONa	1749	HCOOH *vs* DCOOH	1749 / 641 = 2.7
2	DCOOH / DCOONa	641	HCOOH *vs* DCOOD	1749 / 567 = 3
3	DCOOD / DCOONa	567	DCOOH *vs* DCOOD	641 / 567 = 1.1

[a] The experiment requires the prior preparation of a 10:1 mixture of formic acid / sodium formate. Then, a formic acid / sodium formate solution (91 µL, 2.35-2.40 mmol of formic acid) was added to **1d** (0.1 mol% Ir) at 100 ˚C.

3.4. Identification of the Gases Released by Gas Chromatography.

Table S9. GC Analysis of Gases Produced from Dehydrogenation

Entry	[Catalyst] (mol%)	HCOOH (mmol)	Solvent	Additive (mol%)	Temp. (ºC)	Channel 1[a] (%H_2)	Channel 2[b] (% CO_2)
1	**1a** (1)	0.264	toluene (1 mL)	NEt_3 (11)	70	0.7	100
2	**2** (1)	0.264	toluene (1 mL)	NEt_3 (11)	70	1.7	100
3	**1d** (0.1)	2.35	-	HCOONa (10)	100	5.3	100
4	**1d** (0.02)	2.35	-	HCOONa (10)	90	0.6	100

[a] N_2, O_2, CO and H_2 are measured by channel 1; N_2 and O_2 are present in the samples; CO values below the limit. [b] CO_2 is measured by channel 2.

4. Reaction profiles

4.1. Dehydrogenation of Formic Acid in Solution

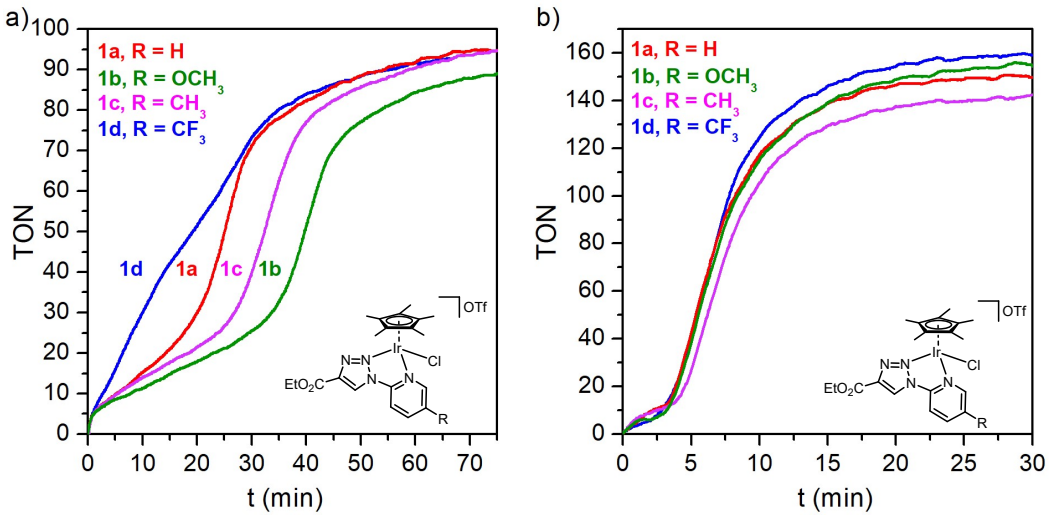

Fig. S1. TON vs time for the dehydrogenation of HCOOH (10 µL, 0.264 mmol) in toluene (1 mL) with NEt_3 (11 mol%) (a) at 70 °C in the presence of 1 mol% of catalysts **1a-1d** and (b) at 90 °C in the presence 0.5 mol% of **1a-1d**.

Dehydrogenation of Formic Acid catalysed by [Cp*Ir(CO)H_2] (2)

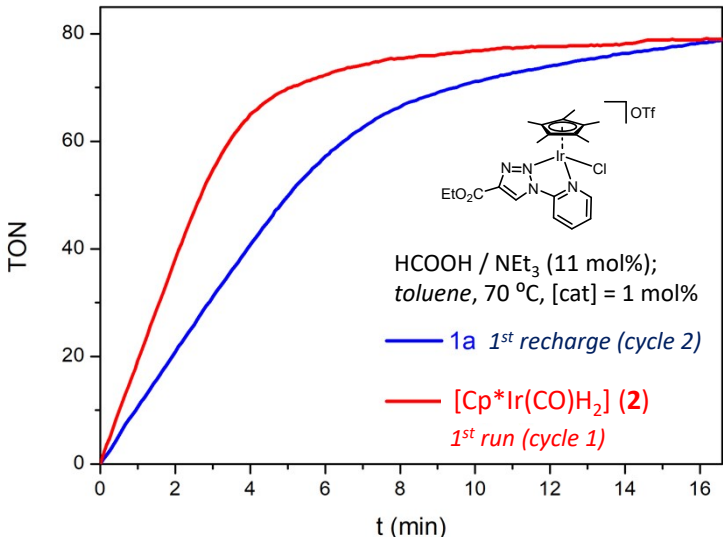

Fig. S2. Comparison of the reaction profiles for the dehydrogenation of formic acid in toluene using (a) catalyst [Cp*Ir(CO)H_2] (**2**) (**Red plot**,) and (b) catalyst **1a** (**Blue plot,** corresponding to entry C2 in Table S3). The remaining conditions were identical in both cases: 1 mol% of catalyst, HCOOH (10 µL, 0.264 mmol), NEt_3 (11 mol%), toluene (1 mL) at 70 °C.

4.2. Dehydrogenation of neat Formic Acid

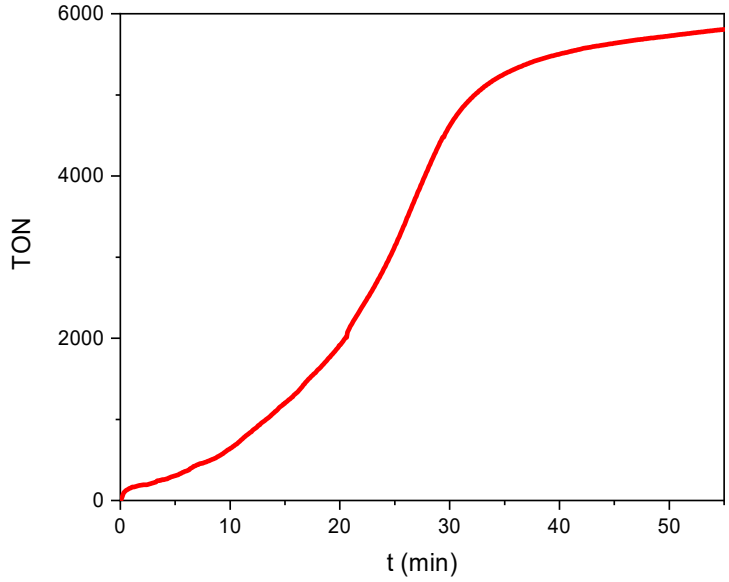

Fig. S3. TON vs time for the dehydrogenation of neat formic acid (100 μL; 2.64 mmol) / NEt_3 (39 μL; 11 mol%) using catalyst **1a** (0.01 mol%) at 100 ˚C.

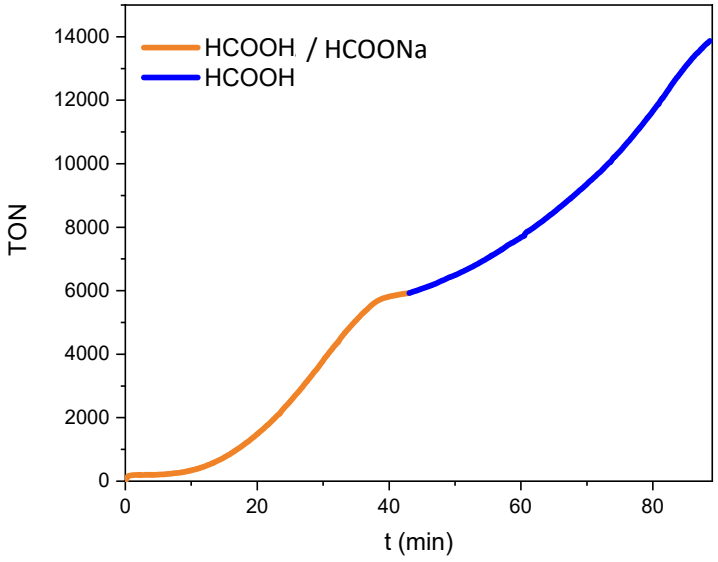

Fig. S4. TON vs time for the dehydrogenation of neat formic acid over two runs, at 90 °C. (i) Dehydrogenation of a 10:1 mixture HCOOH/HCOONa (2.35 mmol of HCOOH) using catalyst **1d** (0.01 mol%) (**orange plot**); (ii) Subsequent addition of neat HCOOH (2.64 mmol) (**blue plot**).

5. Catalysis at the NMR Scale

5.1. Dehydrogenation of HCOOH catalysed by 1a at the NMR scale

Experimental procedure. In a Young NMR tube, **1a** (5.16 mg, 0.007 mmol, 5 mol%), NEt_3 (2.02 μL, 0.025 mmol, 11 mol%) and mesitylene (2.02 μL, 0.014 mmol, 10 mol%) as internal standard, were dissolved in toluene-d_8 (0.5mL). Then, HCOOH (5 μL, 0.145 mmol) is added at room temperature. The progress of the reaction is monitored by NMR at 65 ˚C.

Interpretation of the ^{1}H NMR spectra. Fig. S5a shows the most informative regions of the seven ^{1}H NMR spectra recorded during the first hour of reaction. In this set of spectra, resonances from up to five different iridium pentamethylcyclopentadienyl complexes (labeled as **A**-**E** in Fig. S5) were observed in addition to those corresponding to the release of the free pyridyl-triazole ligand **La**.

The initial spectrum (spectrum 1) primarily displays the resonances of complex **A**, identified by a Cp* singlet at 1.39 ppm and a characteristic low-field signal for the triazole proton of the coordinated ligand **La**. This indicates that complex **A** retains the intact [Cp*Ir(*NN*)] fragment and likely results from minor alterations in the coordination sphere of complex **1a** upon dissolution in the HCOOH/NEt_3 toluene solution (complex **1a** is poorly soluble in toluene), which includes the consideration of a η^1-coordination mode for the pyridyl-1,2,3-triazole ligand.[7]

After 17 minutes of reaction (spectrum 3), the resonances of four hydride Cp*IrH_n complexes are clearly visible: **B** (Cp* at 1.60 ppm, Ir-H at −12.63 ppm), **C** (Cp* at 1.60 ppm, Ir-H at −13.27 ppm), **D** (Cp* at 1.71 ppm, Ir-H at −15.43 ppm), and **E** (Cp* at 1.94 ppm, Ir-H at −16.02 ppm). The formation of these hydride complexes is associated with the decoordination of the ligand **La**, as shown in Fig. S5b, where the total concentrations of hydride complexes and free ligand are compared.

The concentration of the hydride complexes **B** and **C** increases rapidly during the first 20 minutes, but decreases rapidly thereafter, corresponding with the formation of complexes **D** and **E** (Fig. S5c). The coupling between the Cp* ring and the hydride protons is small (< 1 Hz) but sufficient to predict the number of hydride groups in the complexes from the shape of the Cp* resonance envelope (see detail for complex **E** in spectrum 7 and Fig. S7). Based on this, **B** and **D** would be [Cp*IrH] monohydride complexes and **C** and **E** [Cp*IrH_2] dihydride complexes. In fact, complex **E** has been characterized as the previously reported dihydride carbonyl complex [Cp*Ir(CO)H_2] (**2**);[2] see main text and section 2.3 of this SI. This dihydride complex predominates after 40

minutes (spectrum 7 and Fig. S5d) and becomes the only Cp*Ir complex observed in the reaction medium after 18 hours (Fig. S9a).

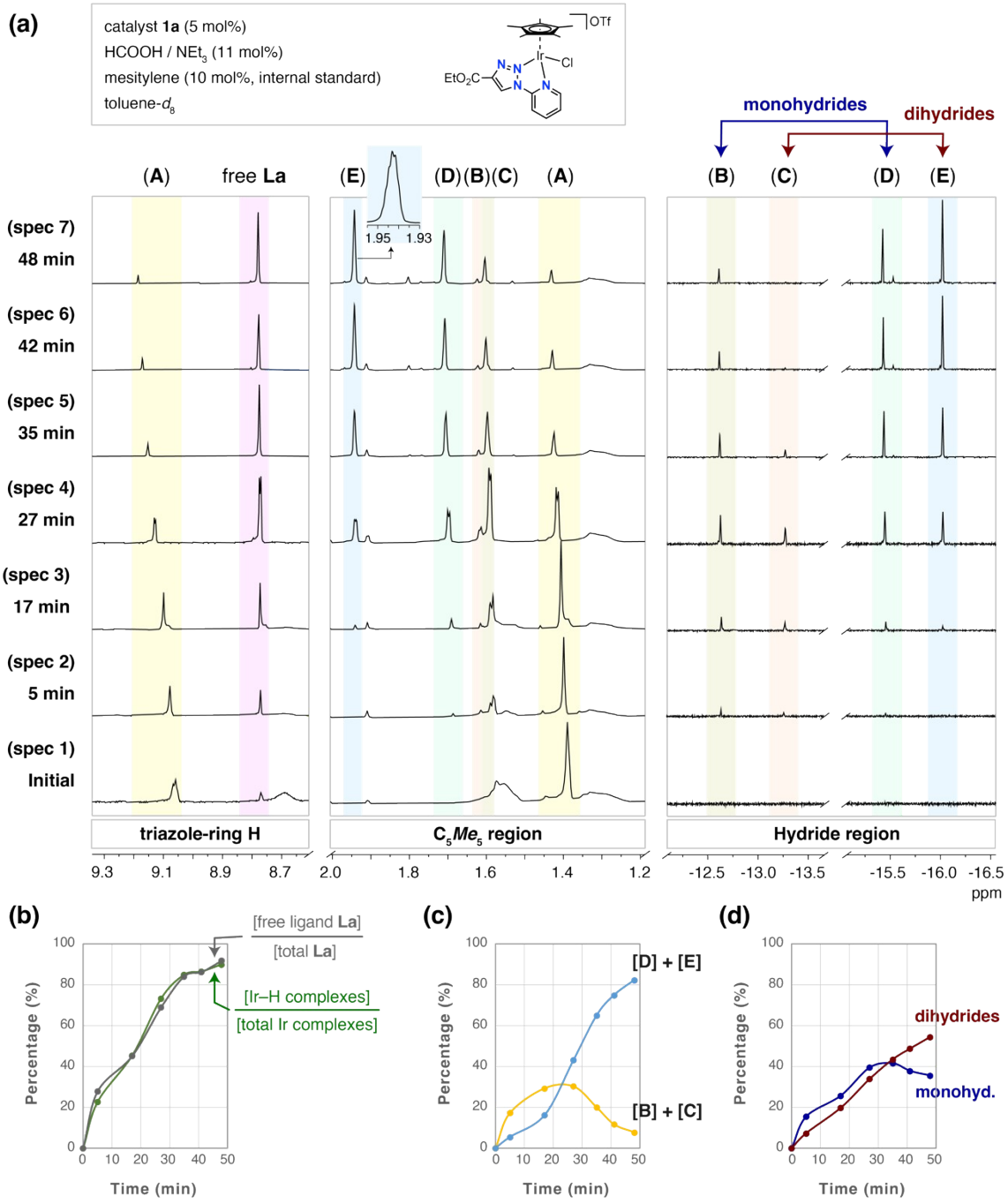

Fig. S5. (a) ^{1}H NMR spectra (500 MHz, toluene-d_8, 338 K) recorded during the dehydrogenation of formic acid using catalyst **1a** (5 mol%) and NEt_3 (11 mol%). Mesitylene (10 mol%) was added as an internal standard. The vertical scale of each region has been modified independently for easier visualization. (b) Evolution over time of the percentage of free ligand with respect to the total amount of **La** (free + coordinated) is compared with that of the percentage of hydride complexes in the total amount of iridium complexes. (c) Evolution over time of the total concentration of the hydride complexes **B** and **C** in comparison with that of the complexes **D** and **E**. (d) Evolution over time of the total concentration of the supposed monohydride complexes **B** and **D** in comparison with that of the dihydride complexes **C** and **E**.

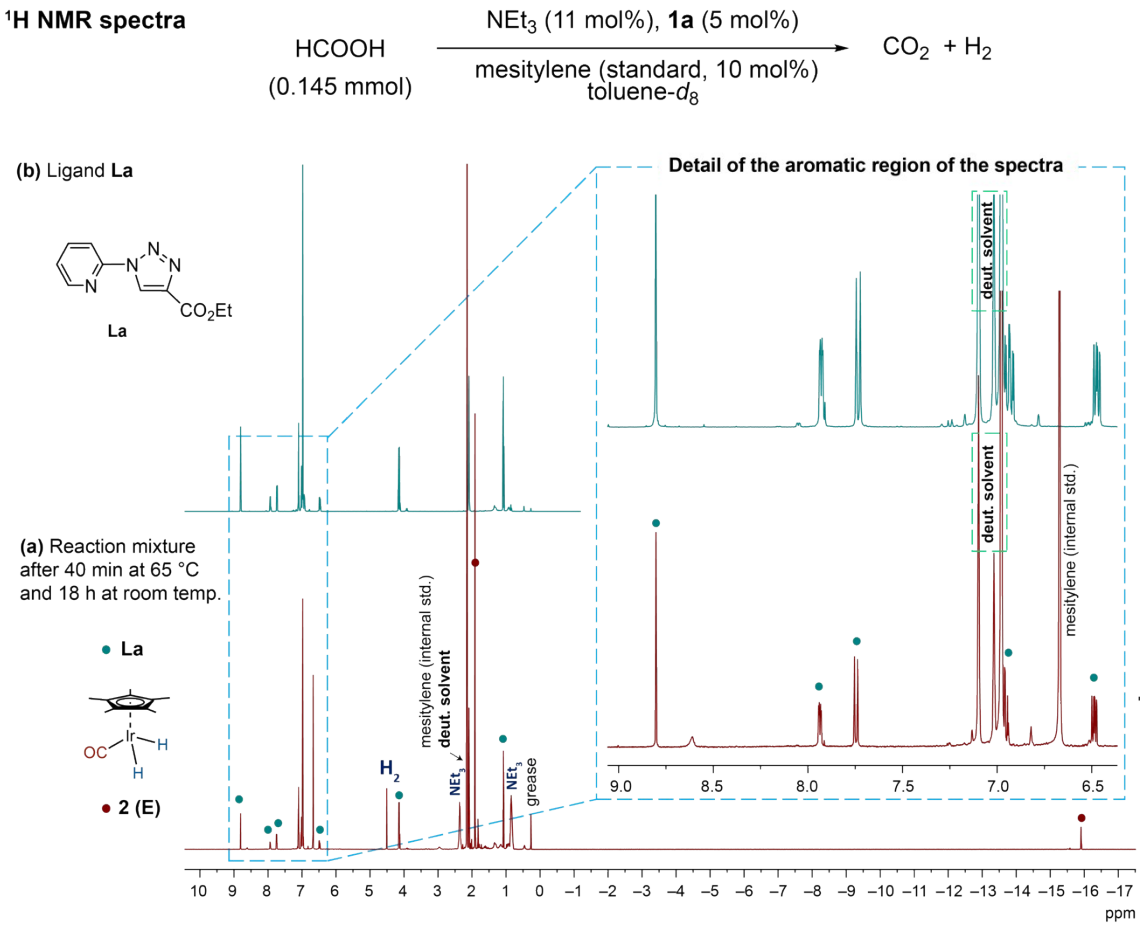

Fig. S6. The ^{1}H NMR spectrum (500MHz, toluene-d_8, 298K) of the mixture of formic acid, triethylamine and catalyst **1a** after 40 min of reaction at 65 ˚C, followed by 18 h at room temperature (a), is compared with the spectrum of ligand **La**. The reaction mixture (a) contains only uncoordinated ligand (●). Furthermore, the only organometallic species observed in (a) is hydride **E** (●), which exhibits ^{1}H resonances at 1.91 ppm for Cp* and at −15.91 ppm for Ir-H. This complex has been characterized as the dihydride carbonyl complex **2** represented in (a). Conditions: HCOOH (0.145 mmol), NEt_3 (11 mol%), **1a** (5 mol%) and mesitylene (10 mol%) as an internal standard.

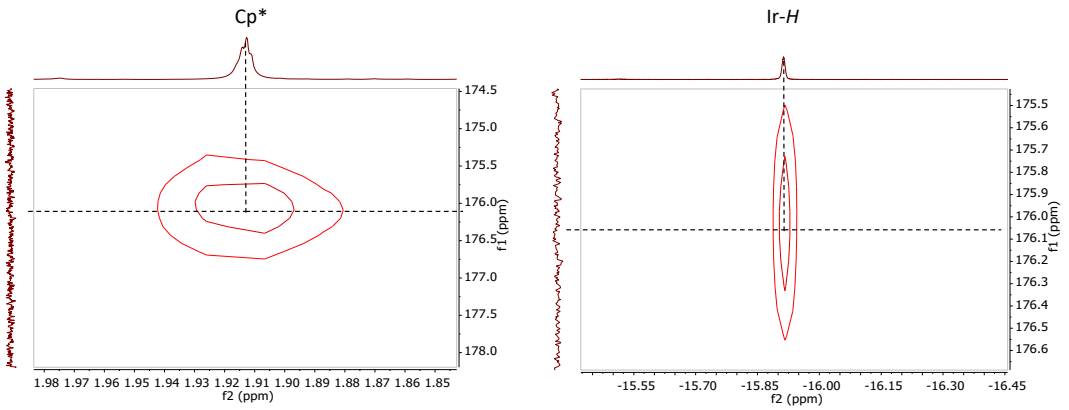

Fig. S7. Detail of the ^{1}H ^{13}C HMBC spectrum (500MHz, toluene-d_8, 298K) corresponding to the mixture: HCOOH (0.145 mmol), NEt_3 (11 mol%) and **1a** (5 mol%) after 40 min at 65 °C, followed by 18 h at room temperature. Evidence for the formation of the dihydride [Cp*Ir(CO)H_2] (**2**).

5.2. Dehydrogenation of HCOOH catalysed by 1d at the NMR scale

Complex **1d** (5.58 mg, 0.007 mmol, 5 mol%) and mesitylene (1 µL; 0.007 mmol, 5 mol%) are placed in a Young NMR tube and dissolved in toluene-d_8 (0.5mL) (Fig. S8a). Subsequently, NEt_3 (2.02 µL, 0.025 mmol, 11 mol%) is added, and the sample is heated at 70 °C for 15 min (Fig. S8b). Finally, HCOOH (5 µL, 0.145 mmol) is added and the mixture heated at 70 °C for 2h. The progress of the reaction is monitored by ^{1}H NMR (measurements taken at room temperature) (Fig. S8).

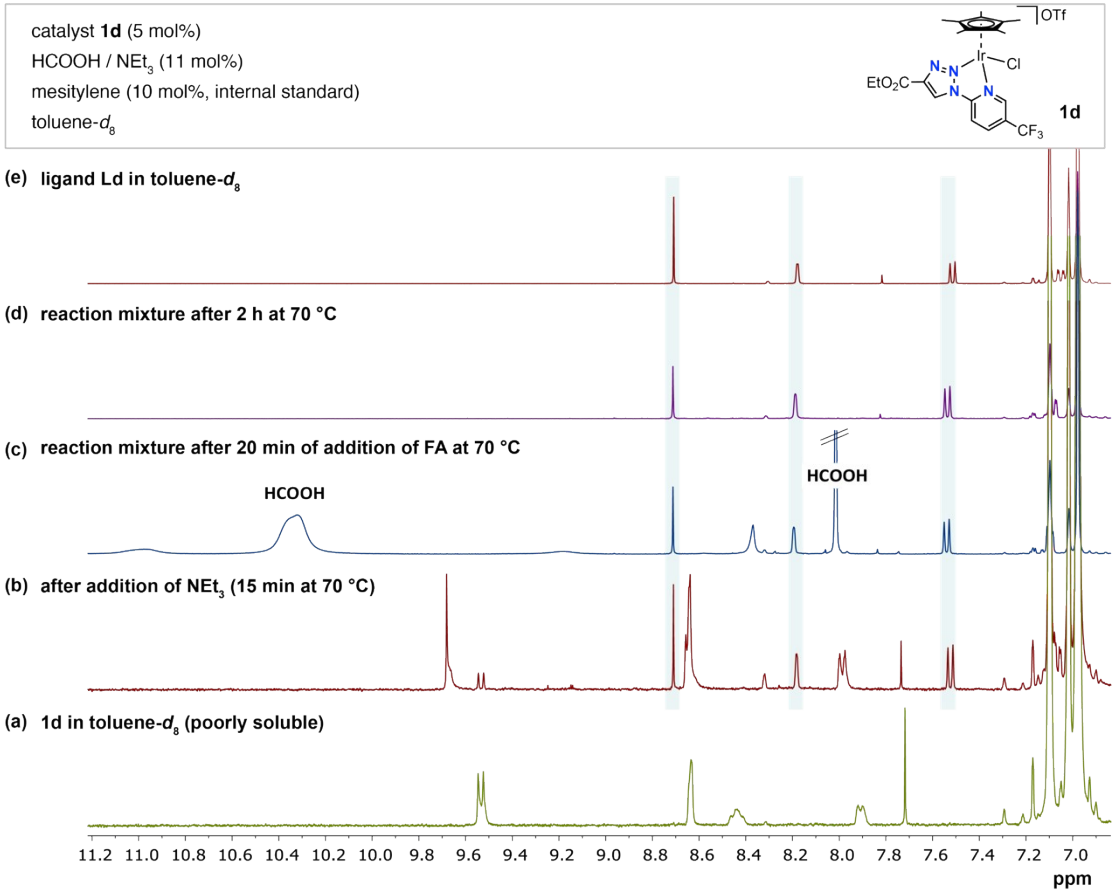

Fig. S8. Detail of the aromatic region of a series of ^{1}H NMR spectra (500MHz, toluene-d_8, 298K) corresponding to the dehydrogenation of formic acid (0.145 mmol) using catalyst **1d** (5 mol%), NEt_3 (11 mol%), and mesitylene (10 mol%) as an internal standard. (a) Initial spectrum of complex **1d**; (b) spectrum after adding NEt_3 (15 min at 70 °C); (c) spectrum after addition of HCOOH (20 min at 70 °C); and (d) spectrum of the reaction mixture after 2h at 70 °C). (e) Spectrum of the free ligand **Ld**.

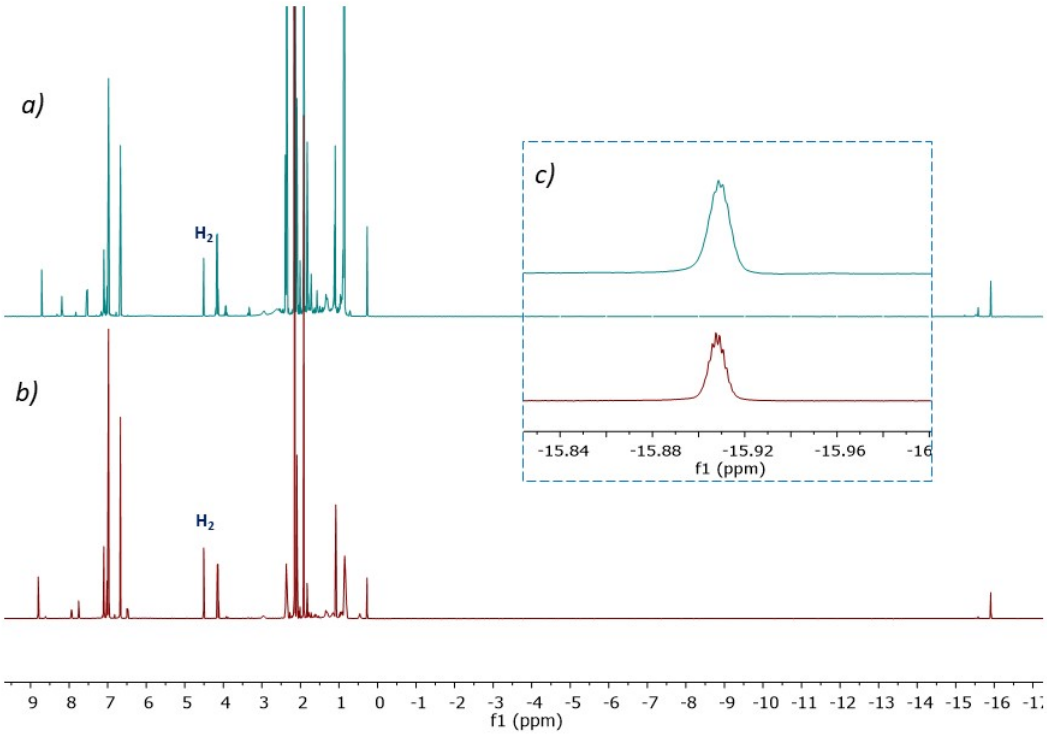

Fig. S9. ^{1}H-RMN (400 MHz, toluene-d_8, 298K). Comparative analysis of the final ^{1}H NMR spectra corresponding to catalytic dehydrogenation of formic acid conducted with complexes **1a** (a) and **1d** (b) at the NMR scale. (c) Comparison of the hydride region for both experiments.

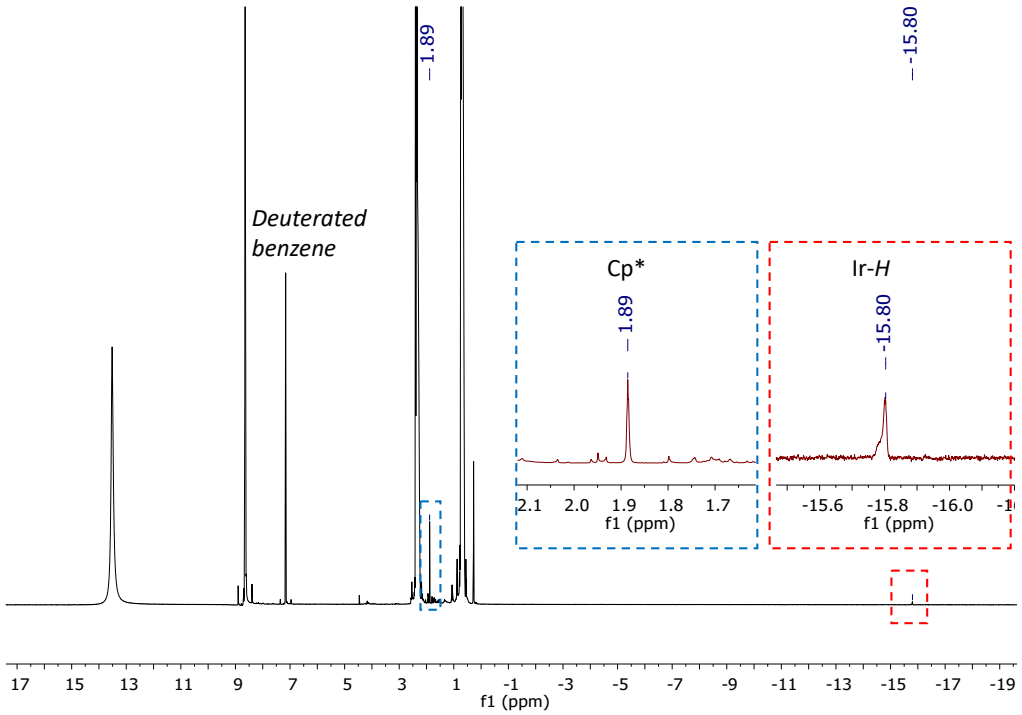

Fig. S10. ^{1}H NMR spectra (400MHz, C_6D_6, 298K) corresponding to the residue of the catalytic dehydrogenation of neat HCOOH (100 µL, 2.64 mmol), with NEt_3 (39 µL,11 mol%) using **1d** (2.64 x 10^{-3} mmol, 0.1 mol%) 1 hour at 100 °C and an additional 1 hour at room temperature.

6. NMR and Mass Spectra

6.1 Ligands Lc and Ld

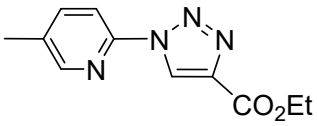

Lc

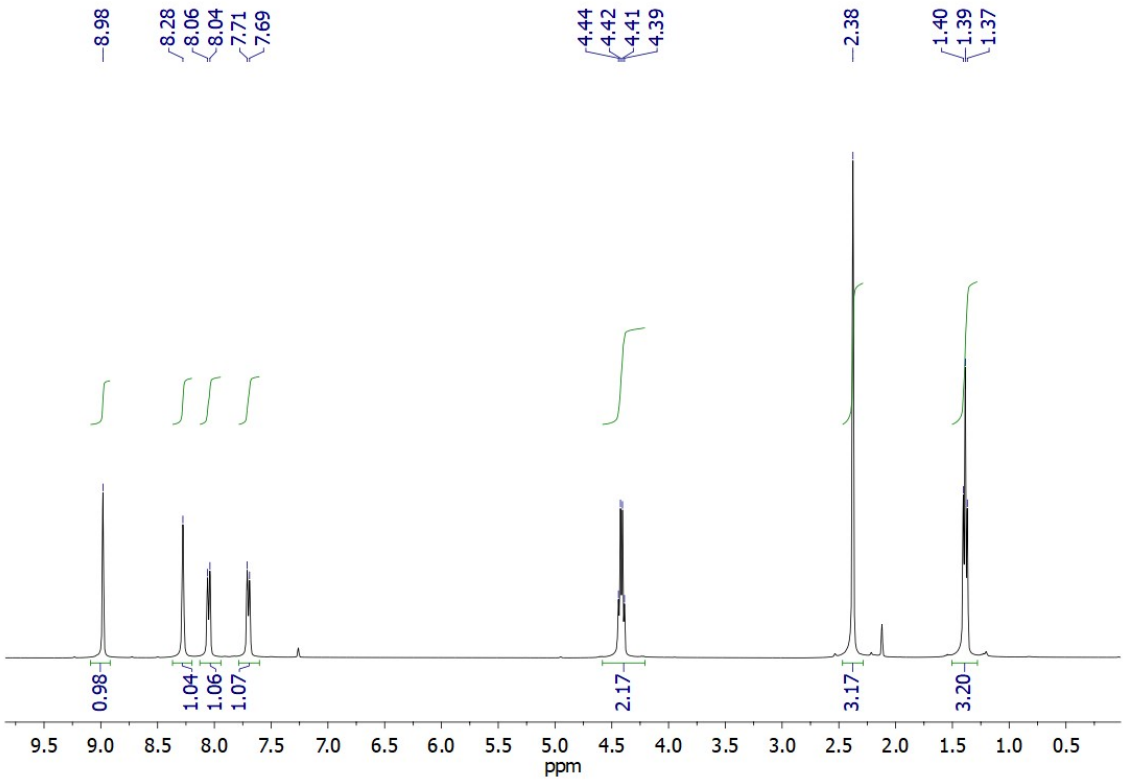

Fig. S11. ^{1}H NMR (400MHz, $CDCl_3$, 298K) spectrum of Ligand **Lc**.

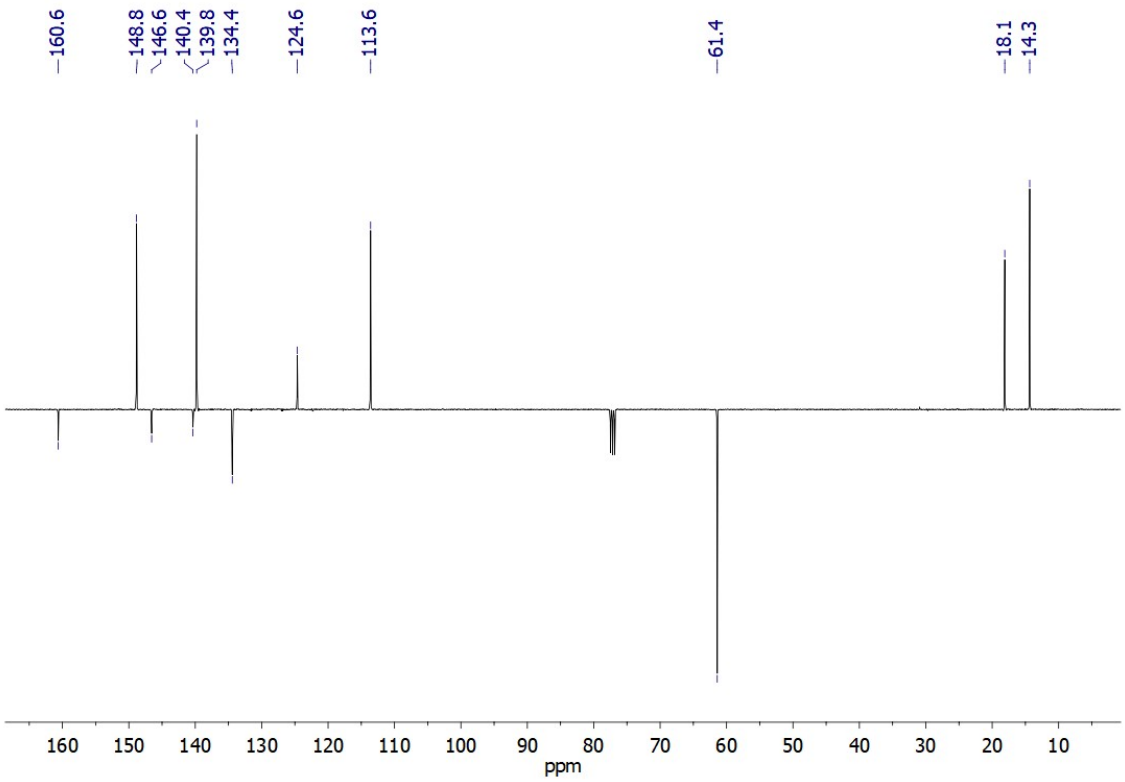

Fig. S12. $^{13}C\{^{1}H\}$-APT NMR (101MHz, $CDCl_3$, 298K) spectrum of Ligand **Lc**.

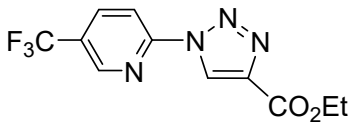

Ld

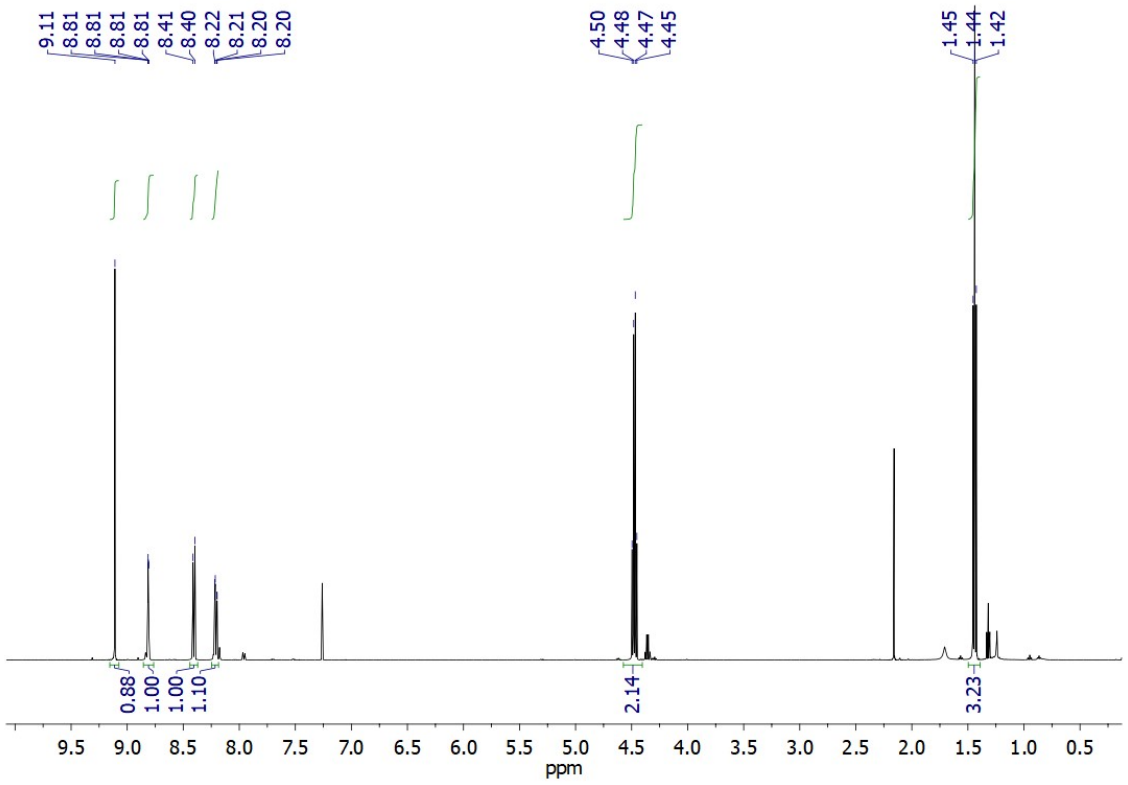

Fig. S13. ^{1}H NMR (400MHz, $CDCl_3$, 298K) spectrum of Ligand **Ld**.

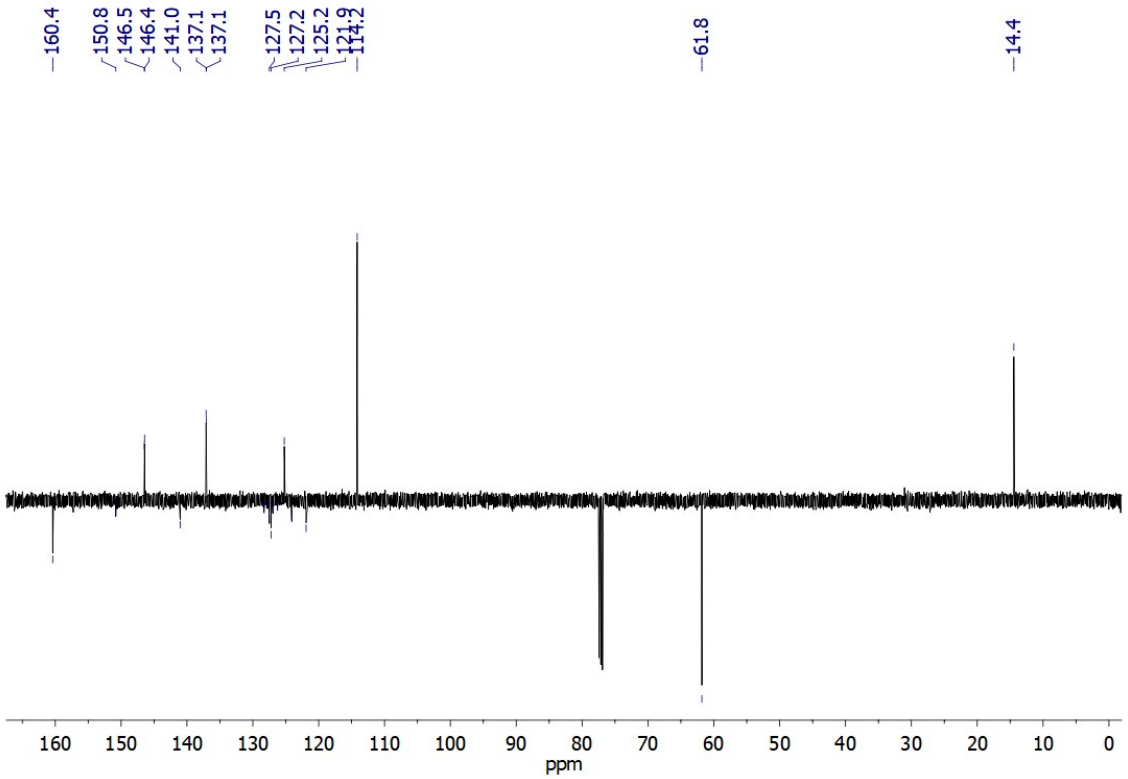

Fig. S14. $^{13}C\{1H\}$-APT NMR (101MHz, $CDCl_3$, 298K) spectrum of Ligand **Ld**.

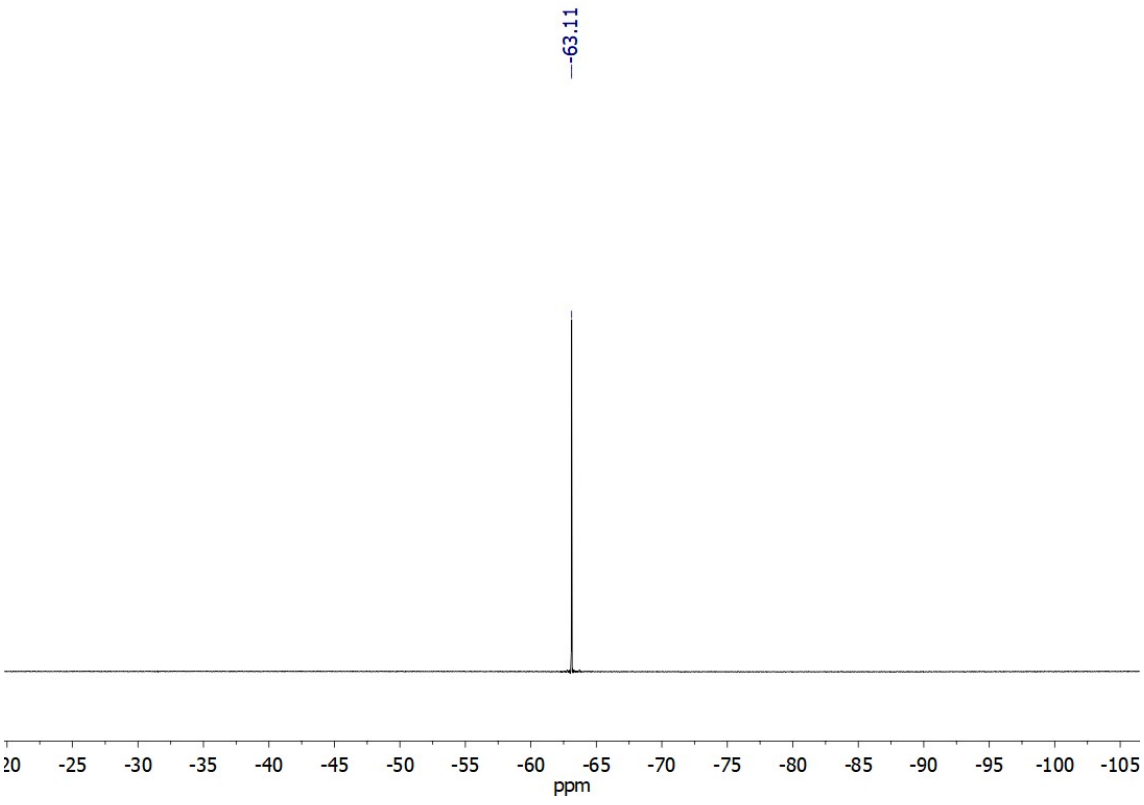

Fig. S15. $^{19}F\{1H\}$ NMR (282MHz, $CDCl_3$, 298K) spectrum of Ligand **Ld**.

6.2 Complexes 1a−1d

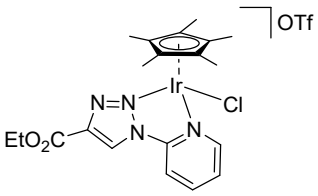

Complex 1a

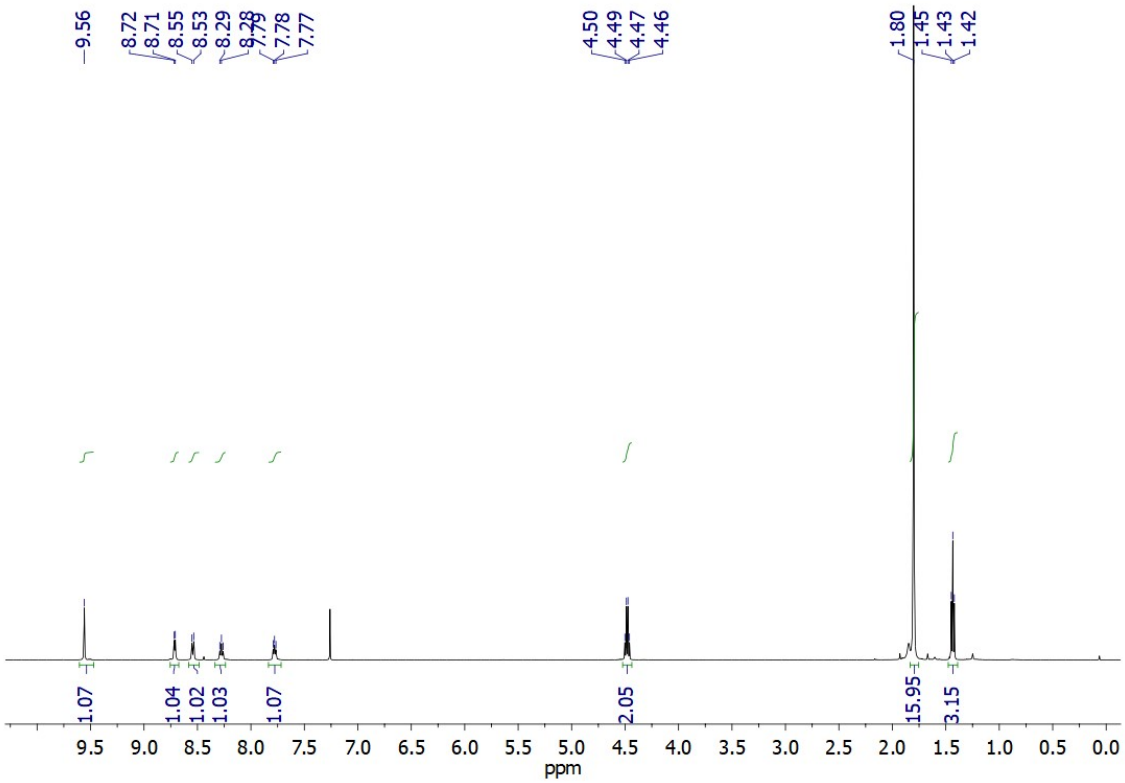

Fig. S16. ^{1}H NMR (500MHz, $CDCl_3$, 298K) spectrum of complex **1a**.

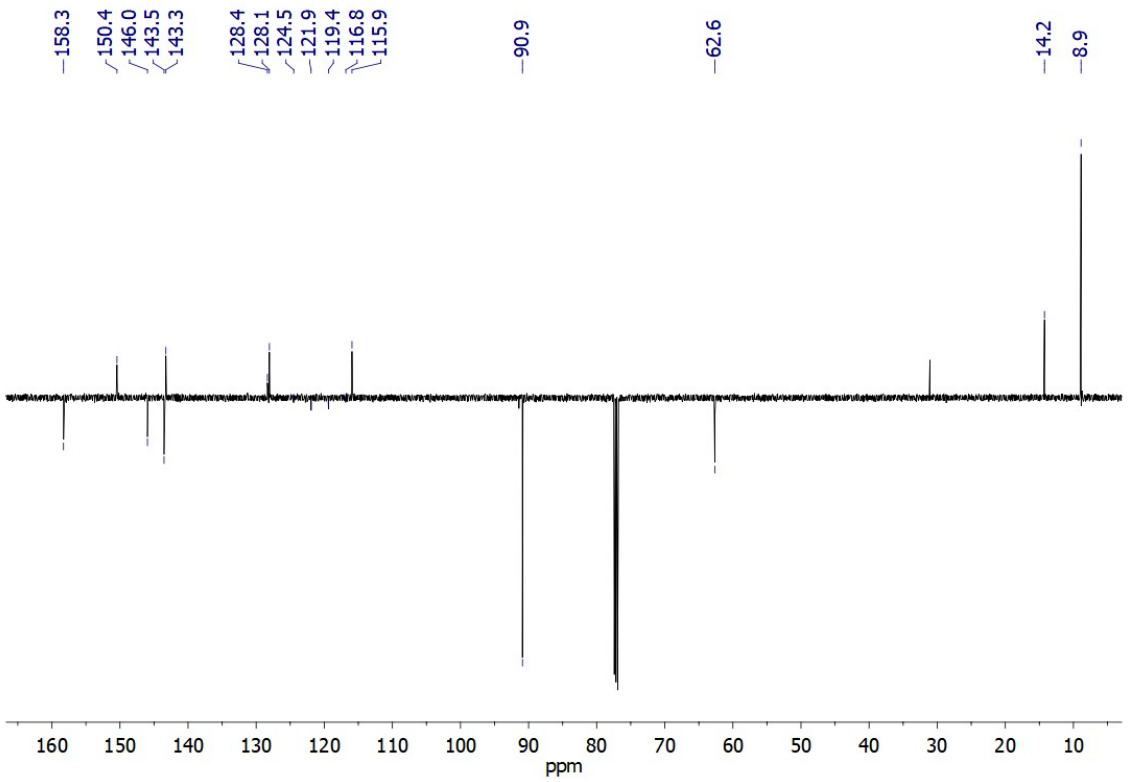

Fig. S17. $^{13}C\{1H\}$-APT NMR (126MHz, $CDCl_3$, 298K) spectrum of complex **1a**.

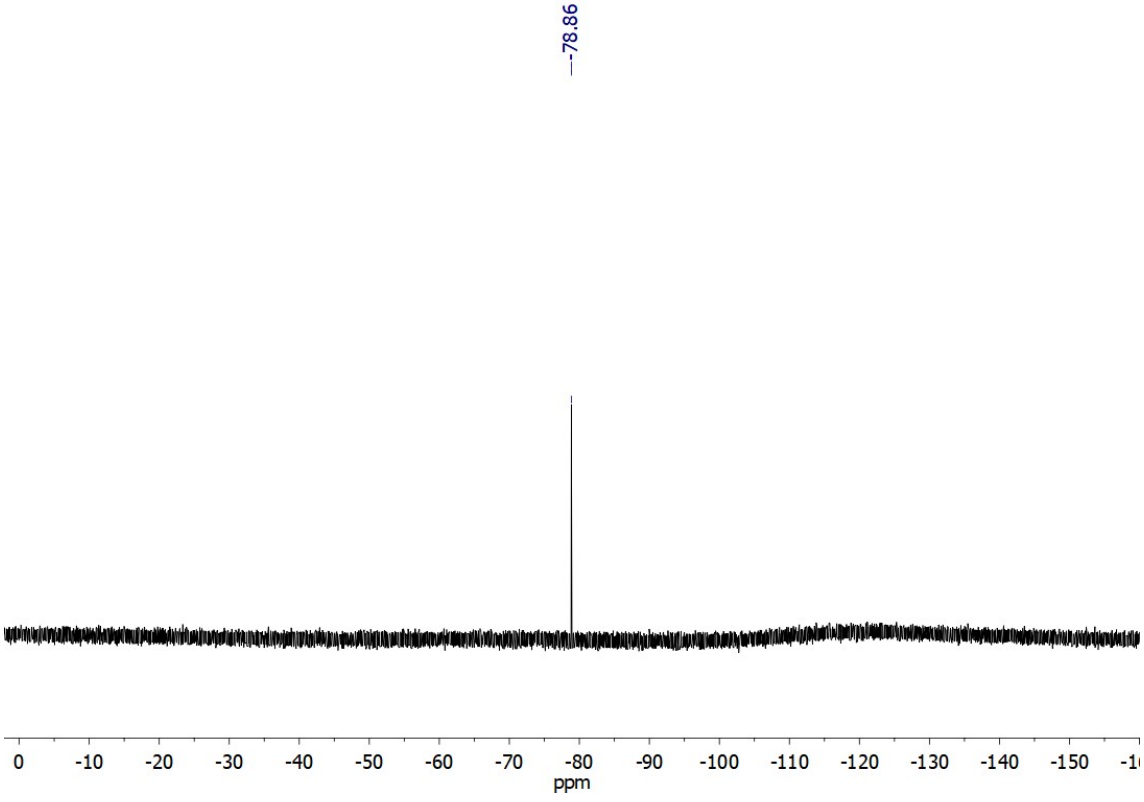

Fig. S18. $^{19}F\{1H\}$ NMR (282MHz, $CDCl_3$, 298K) spectrum of complex **1a**.

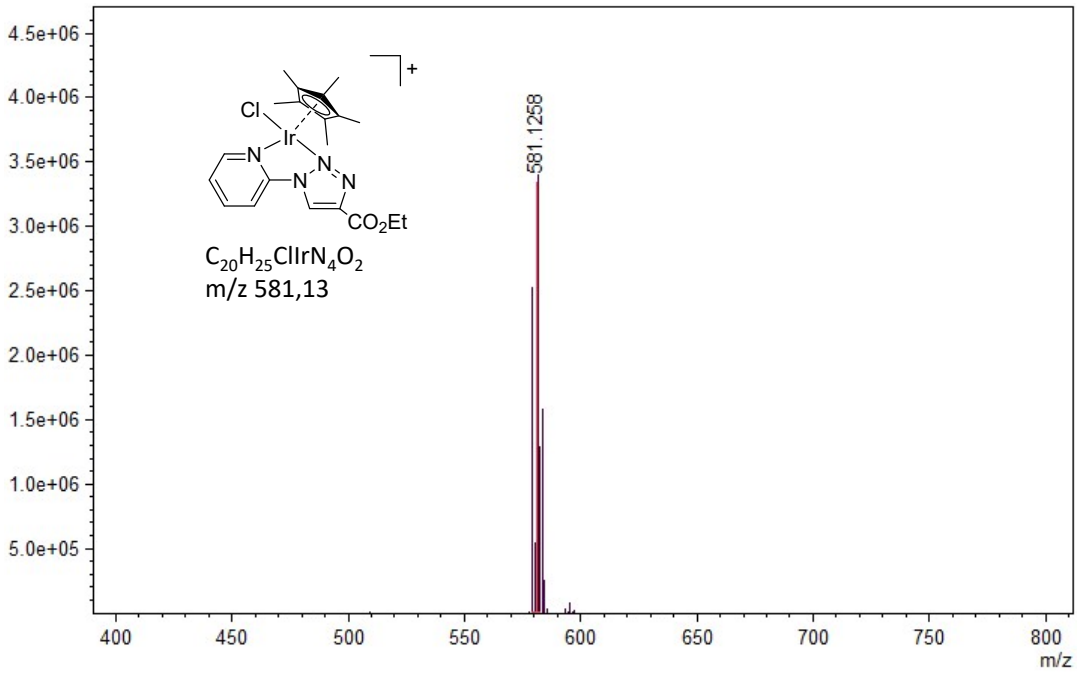

Fig. S19. ESI-TOF(+) mass spectrum of **1a** in dichloromethane.

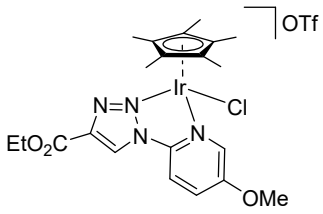

Complex 1b

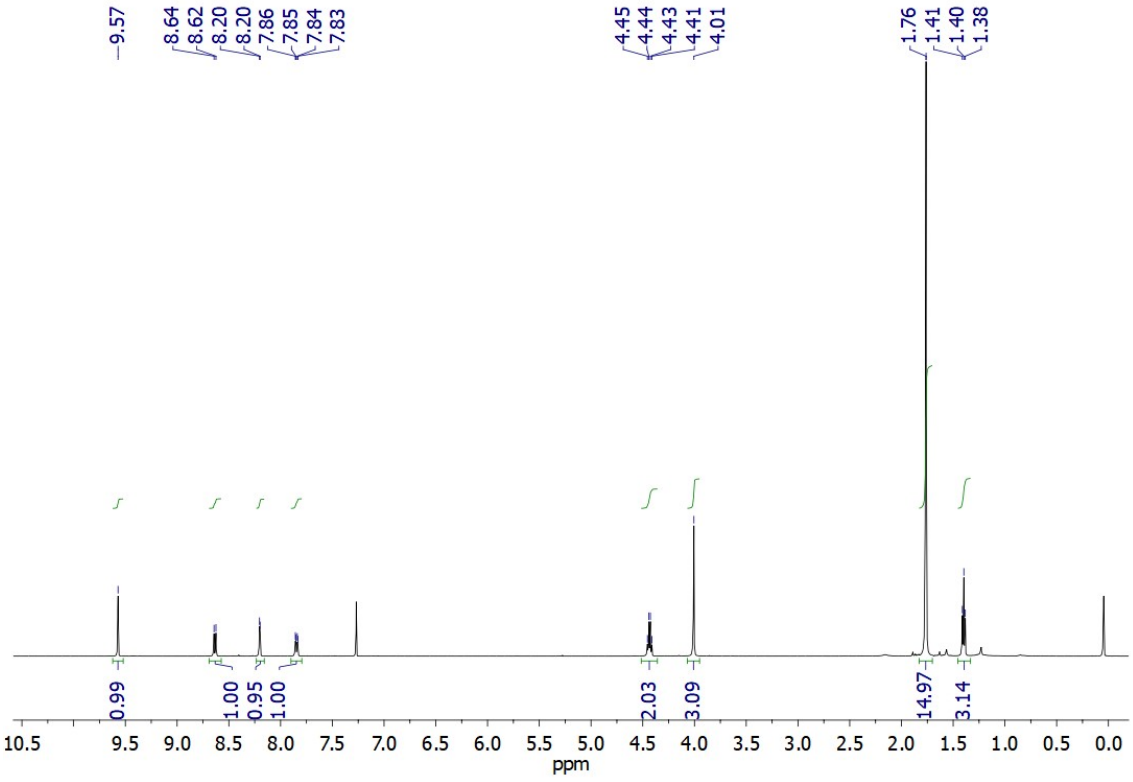

Fig. S20. ^{1}H NMR (500MHz, $CDCl_3$, 298K) spectrum of complex **1b**.

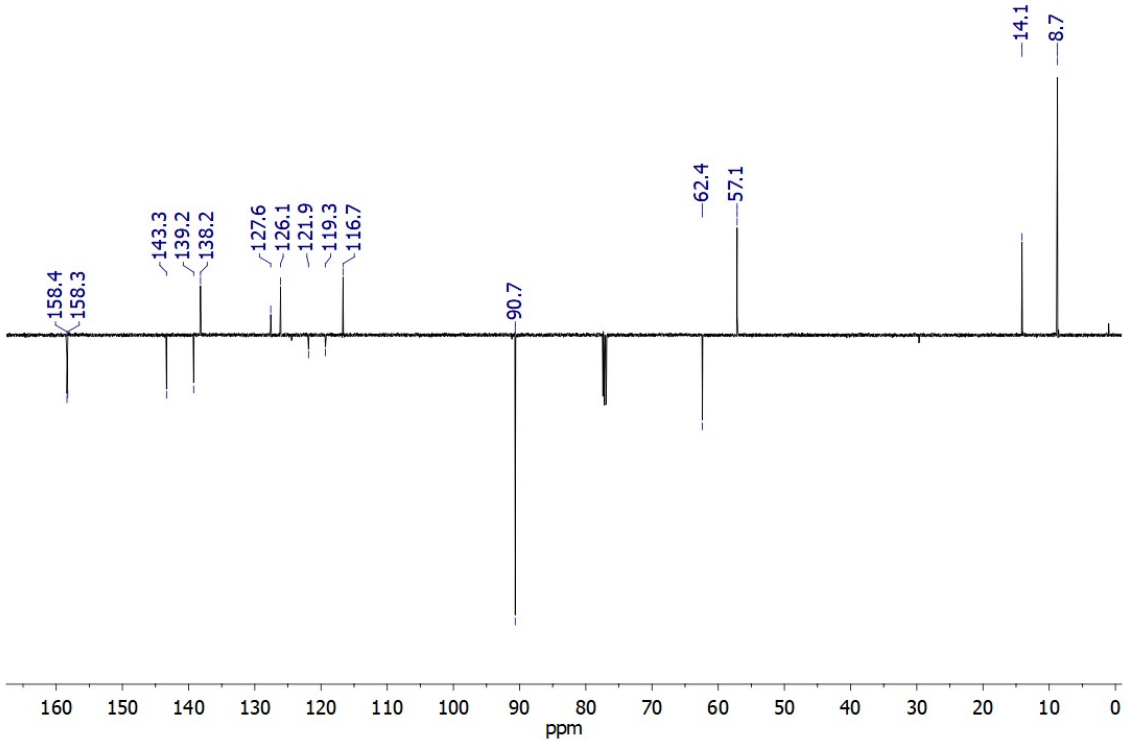

Fig. S21. $^{13}C\{1H\}$-APT NMR (126MHz, $CDCl_3$, 298K) spectrum of complex **1b**.

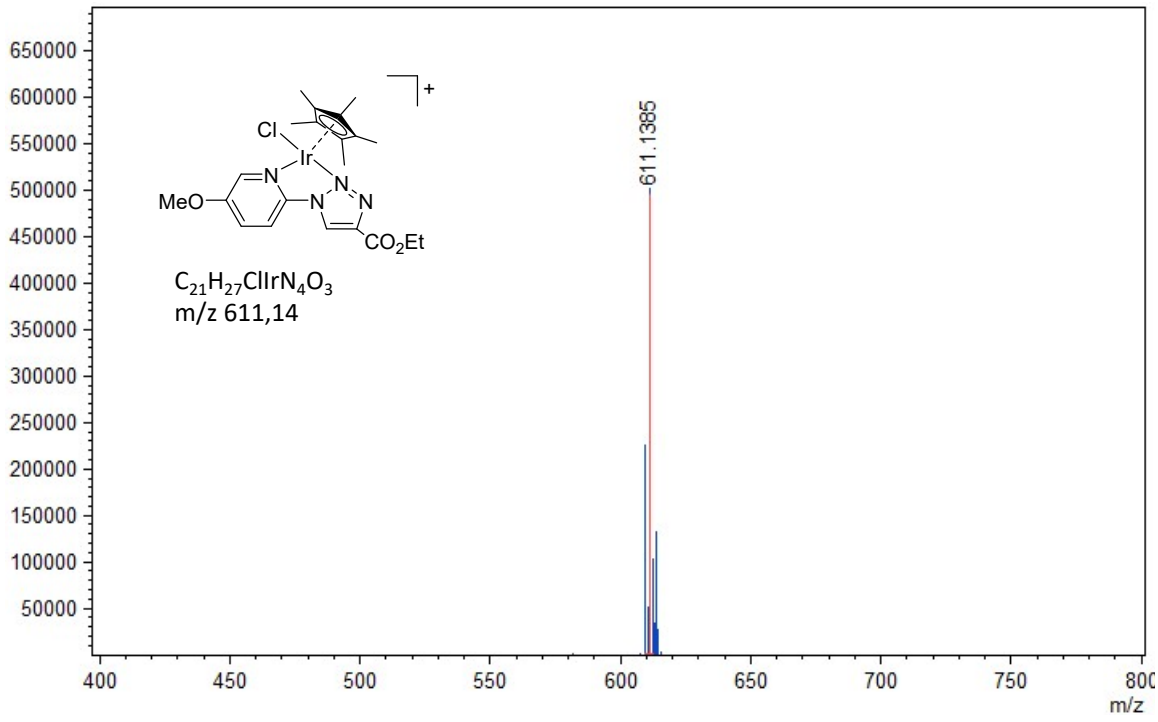

Fig. S22. ESI-TOF(+) mass spectrum of **1b** in dichloromethane.

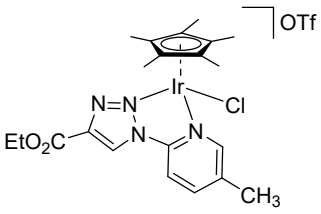

Complex 1c

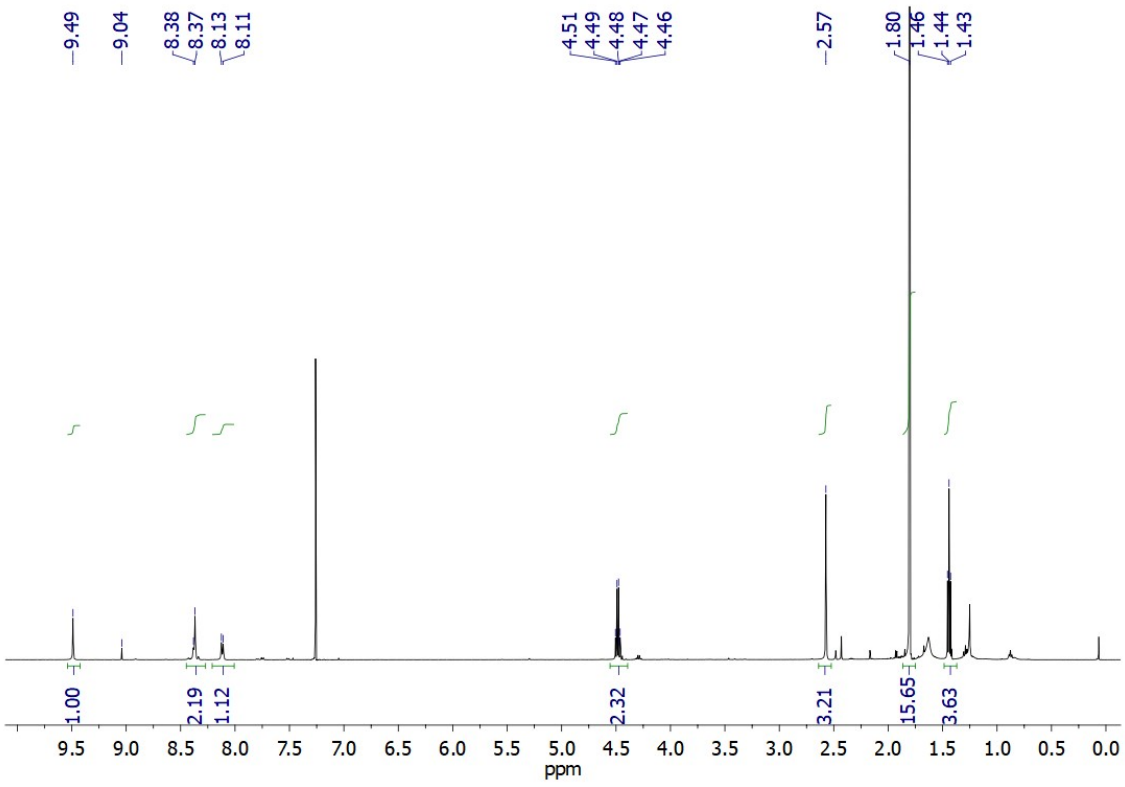

Fig. S23. ^{1}H NMR (500MHz, $CDCl_3$, 298K) spectrum of complex **1c**.

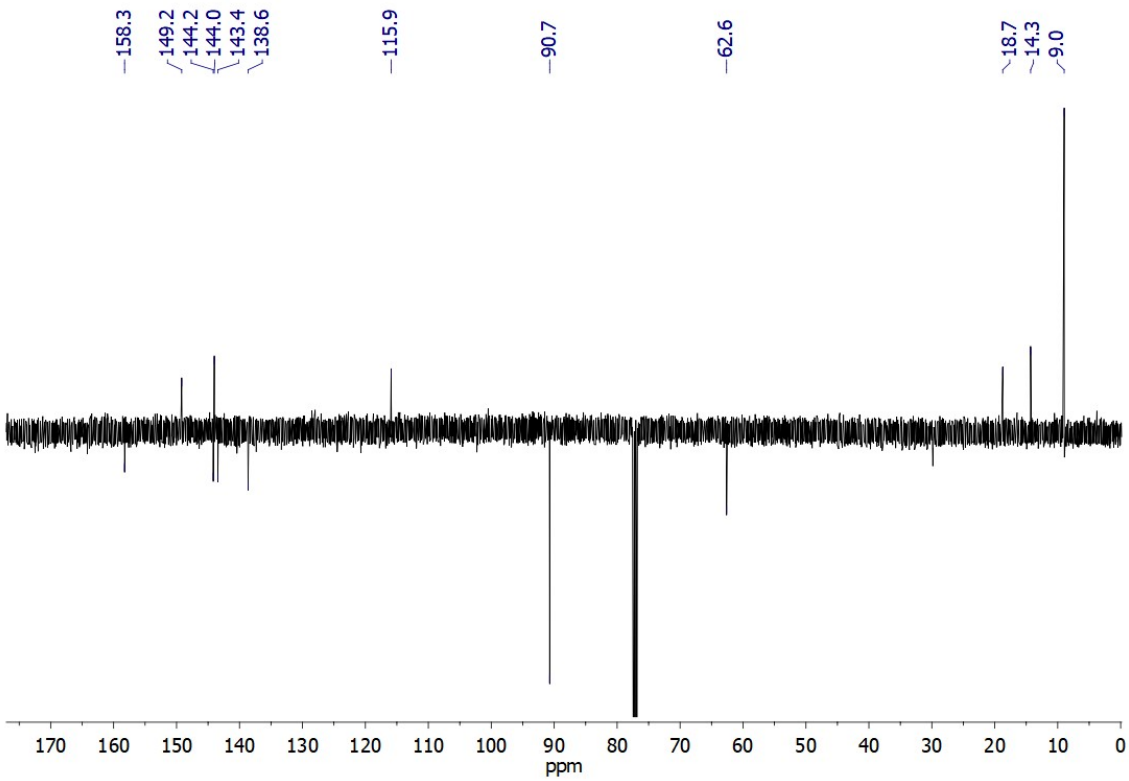

Fig. S24. $^{13}C\{1H\}$-APT NMR (126MHz, $CDCl_3$, 298K) spectrum of complex **1c**.

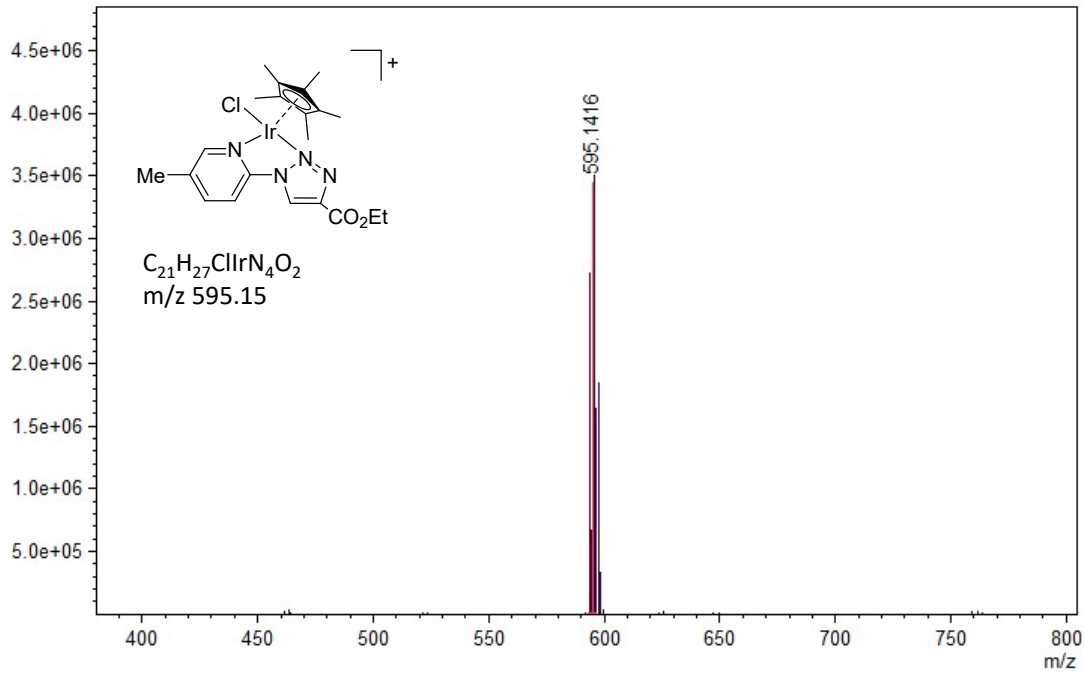

Fig. S25. ESI-TOF(+) mass spectrum of **1c** in dichloromethane.

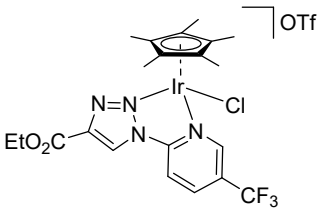

Complex 1d

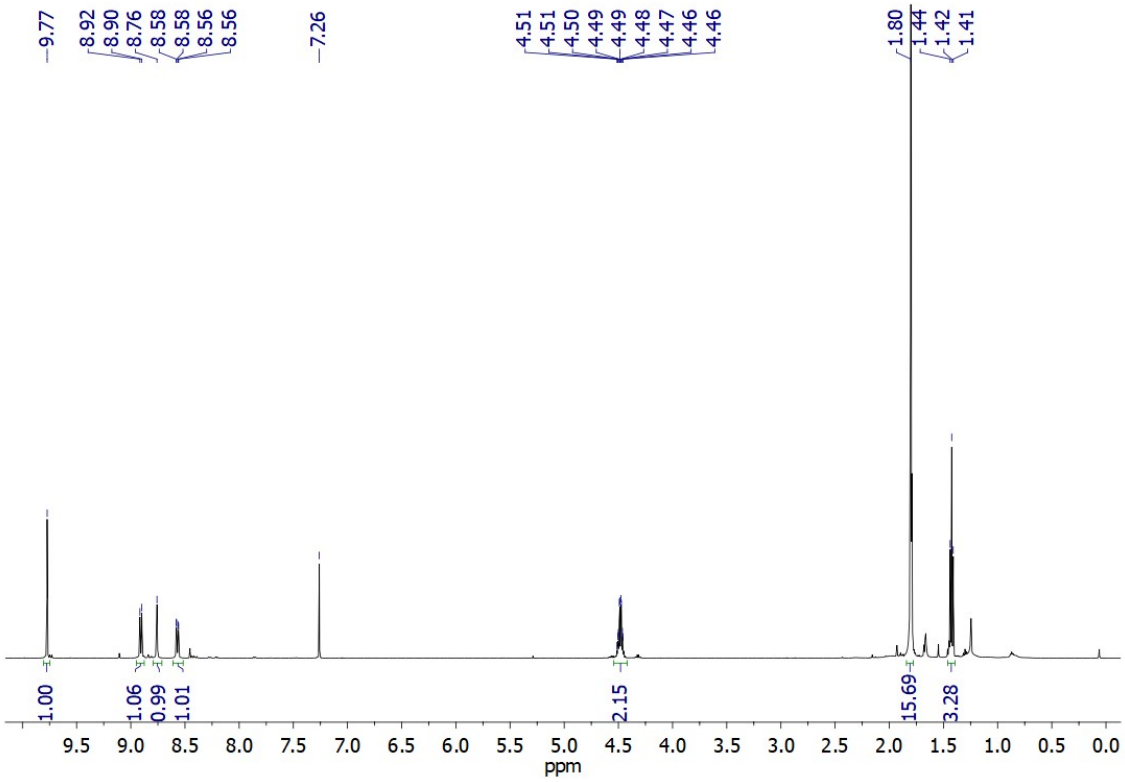

Fig. S26. ^{1}H NMR (500MHz, $CDCl_3$, 298K) spectrum of complex **1d**.

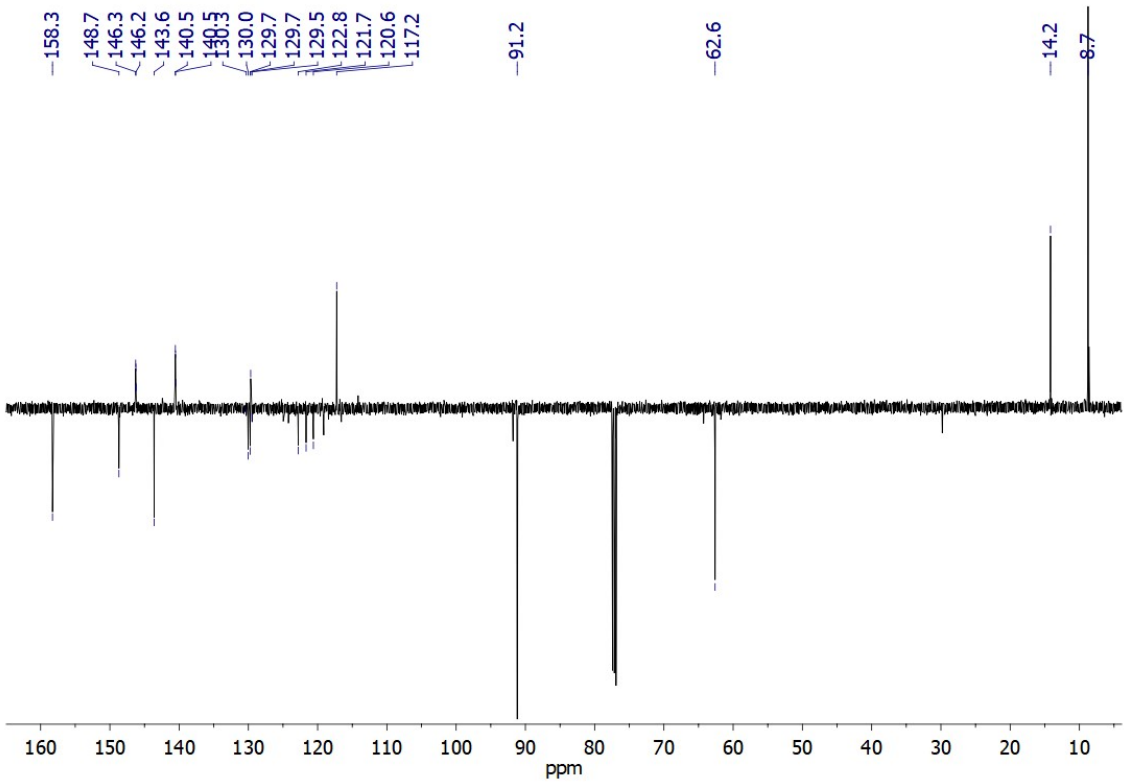

Fig. S27. $^{13}C\{1H\}$-APT NMR (126MHz, $CDCl_3$, 298K) spectrum of complex **1d**.

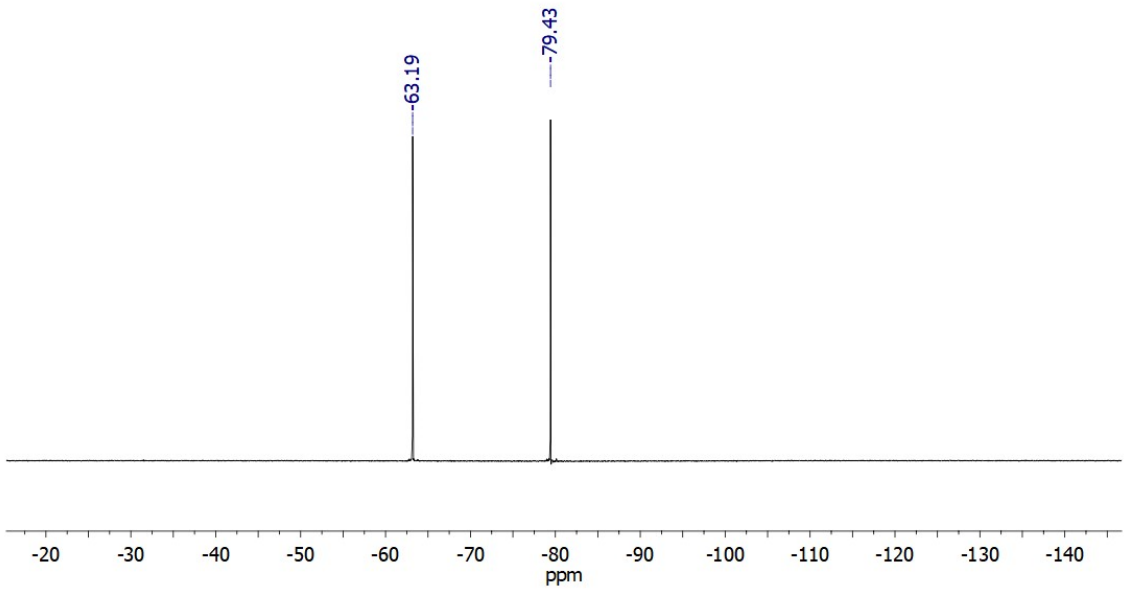

Fig. S28. $^{19}F\{1H\}$ NMR (282MHz, $CDCl_3$, 298K) spectrum of complex **1d**.

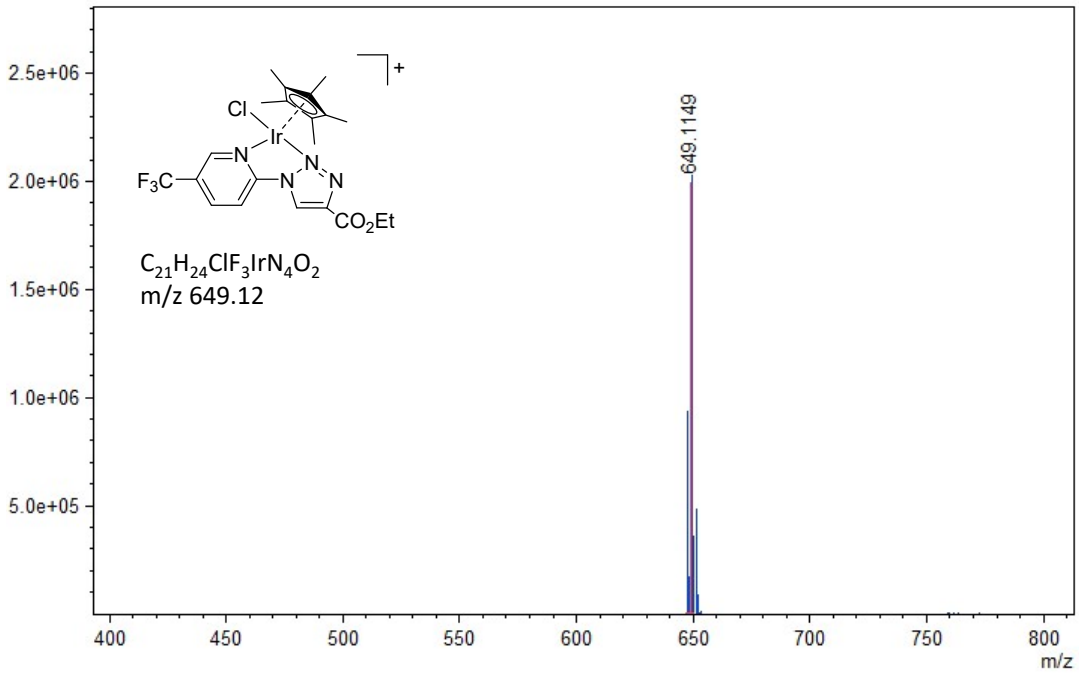

Fig. S29. ESI-TOF(+) mass spectrum of **1d** in dichloromethane.

6.3. Complex [Cp*Ir(CO)H_2] (2)

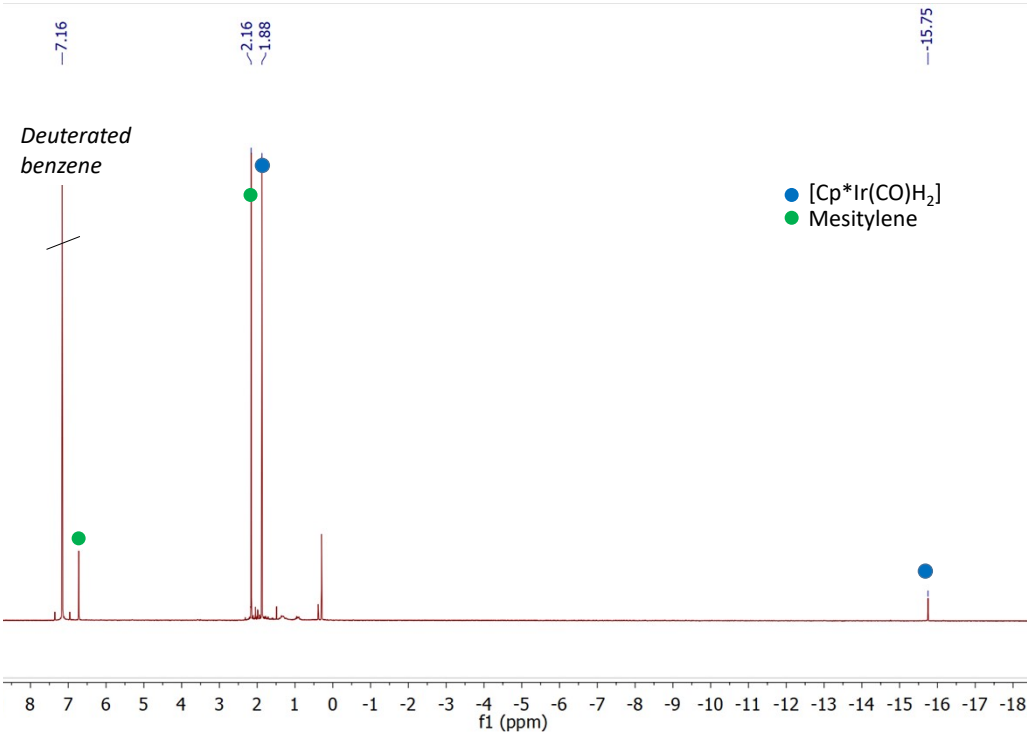

Fig. S30 ^{1}H NMR (400 MHz, C_6D_6, 298K) of [Cp*Ir(CO)H_2] and mesitylene (internal standard).

6.3.1. Hydrogenation of $[Cp^*Ir(CO)]_2$ with H_2. A solution of $[Cp^*Ir(CO)]_2$ in benzene-d_6 (0.4 mL), introduced into a valved J. Young NMR tube, was monitored by ^1H NMR spectroscopy at 298K, under H_2 atmosphere, for two months (Fig. S31).

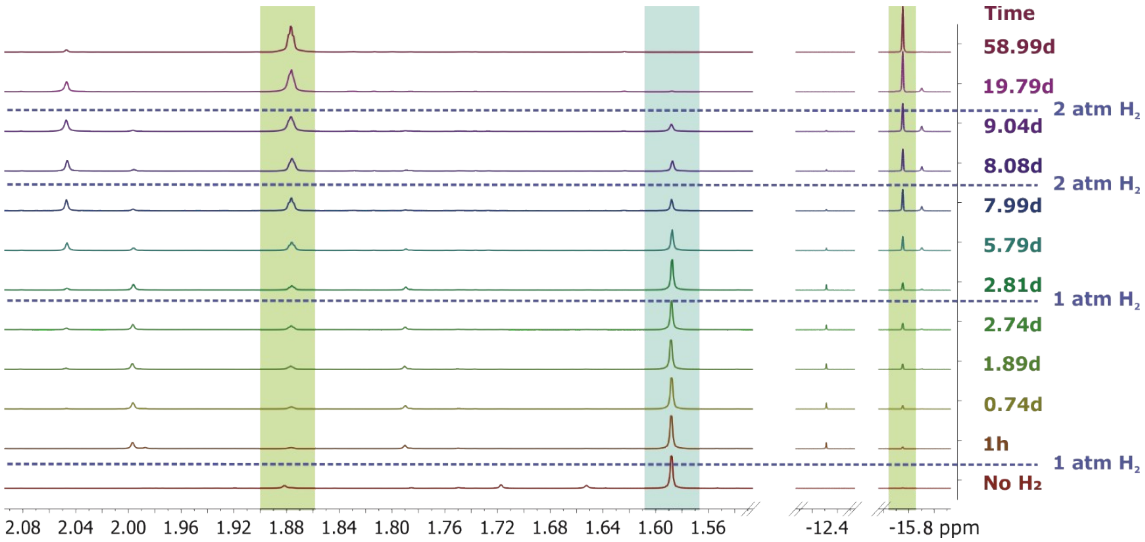

Fig. S31. ^1H NMR monitoring (400MHz, C_6D_6, 298K) of the hydrogenation of the dimer $[Cp^*Ir(CO)]_2$. The left part of the spectra shows the disappearance of the Cp* proton resonance of the dimer and the simultaneous appearance of the Cp* resonance corresponding to complex **2**. On the right, the appearance of the hydride resonance of complex **2** is observed. Additionally, the formation of an intermediate hydride complex is detected.

7. Crystal Structure Determination Details

Suitable single crystals of **1a** were obtained by slow diffusion of diethyl ether into a saturated solution of complex **1a** in dichloromethane. A summary of crystal data, data collection, and refinement parameters for the structural analysis is given in Table S10. Crystals were glued to a glass fiber using an inert polyfluorinated oil and mounted in the low temperature N_2 stream of a Bruker AXS D8 Venture diffractometer with PhotonIII_C14 charge-integrating.

Intensities were collected using graphite-monochromated Mo-Kα radiation (λ = 0.71073 Å). Raw data were corrected for Lorenz and polarization effects. The structure was solved by direct methods, completed by subsequent difference Fourier techniques and refined by full-matrix least squares on F^2 (SHELXL-97).[8] Anisotropic thermal parameters were used in the last cycles of refinement for the non-hydrogen atoms. Absorption correction procedures were carried out using the multiscan SORTAV (semiempirical from equivalent) program. Hydrogen atoms were included in the last cycle of refinement from geometrical calculations and refined using a riding model. All the calculations were made using the WINGX system.[9]

Table S10. Crystal data and structure refinement for 1a.

Empirical formula	$C_{21}H_{25}ClF_3IrN_4O_5S$	
Molecular formula	$[C_{20}H_{25}ClIrN_4O_2]\{[CO_3F_3S]^-\}$	
Formula weight	730.16	
Temperature	200.00 K	
Crystal system	Monoclinic	
Space group	P 2_1/c	
Unit cell dimensions	*a* = 13.1306(17) Å	α = 90°
	b = 11.9213(15) Å	β = 91.022(5)°
	c = 16.014(2) Å	γ = 90°
Volume	2506.3(6) $Å^3$	
Z	4	
Density (calculated)	1.935 g/cm^3	
Absorption coefficient	5.580 mm^{-1}	
F(000)	1424.0	
Crystal size	0.34 mm × 0.3 mm × 0.19 mm	
Radiation	MoKα (λ = 0.71073 Å)	
Theta range for data collection	7.086° to 55°	
Index ranges	$-17 \le h \le 17$, $-15 \le k \le 15$, $-20 \le l \le 20$	
Reflections collected	85095	
Independent reflections	5734 [R_{int} = 0.0527, R_{sigma} = 0.0231]	
Data/restraints/parameters	5734 / 0 / 325	
Goodness–of–fit on F^2	1.063	
Final *R* indices [$I > 2\sigma(I)$]	R_1 = 0.0217, wR_2 = 0.0486	
Final *R* indices (all data)	R_1 = 0.0254, wR_2 = 0.0509	
Largest diff. peak and hole	1.63 and −1.03 e $Å^{-3}$	

8. Computational Details

Calculations were performed at the density functional theory (DFT) level of theory with the Gaussian 09 Rev. D.01 software package[10] and using the M06 functional[11] along with the Def2TZVP[12] basis set for iridium and 6-311G(2df,p)[13] basis set for other atoms. The molecular structures were optimized in gas phase without any symmetry constraint with very tight convergence criteria (optimized coordinates in Table S11). The molecular structure of compound **1a** obtained from X-ray diffraction analysis was used as an initial structural guess for geometry optimization. Frequency calculations were performed at the same level of theory for freely relaxed molecules to distinguish optimized geometries as stationary points on the potential energy surface, which do not exhibit imaginary frequencies. In addition, the stability of the wave functions generated by the self-consistent field (SCF) calculations was checked using the keyword *stable*.

Table S11. DFT-optimized coordinates (M06 / Def2TZVP-6-311G(2df,p)).

O	-4.76773	-0.89206	0.31913	H	1.85423	-0.27828	3.42161
O	-5.28507	1.30122	0.35585	H	3.42563	-1.07006	3.27462
N	-0.94336	0.34656	0.16031	C	0.01826	-2.20546	2.33899
N	-2.06179	-0.27107	0.20250	H	-0.97727	-2.17368	1.88820
Ir	1.03519	-0.30082	-0.09332	H	0.15417	-3.20578	2.76369
Cl	0.70572	0.35353	-2.37707	H	0.04423	-1.48715	3.16045
N	1.13262	1.86181	0.14334	C	0.01316	-3.31514	-0.61184
N	-1.15545	1.68266	0.17724	H	-0.97889	-3.04690	-0.24016
C	2.25731	2.57814	0.06970	H	-0.00959	-3.22743	-1.69978
H	3.18182	2.01116	0.03615	H	0.19642	-4.36503	-0.35962
C	2.25242	3.95454	0.02095	C	2.70288	-2.34612	-2.03433
H	3.18962	4.49361	-0.03601	H	1.85296	-2.51877	-2.69550
C	-0.13286	3.89073	0.08868	H	3.30745	-1.55129	-2.47400
H	-1.10205	4.37432	0.07954	H	3.30743	-3.25978	-2.00846
C	-0.02890	2.51705	0.13820	C	4.31214	-0.55933	0.00133
C	-2.48155	1.90920	0.23135	H	4.52783	0.24181	0.71276
H	-2.93849	2.88546	0.25836	H	5.11044	-1.30176	0.10552
C	-3.04506	0.66134	0.24932	H	4.37594	-0.14918	-1.01039
C	1.03796	4.61975	0.03222	C	-4.50018	0.39637	0.31205
H	1.00048	5.70205	-0.01360	C	-6.16499	-1.25789	0.36224
C	2.24845	-1.14922	1.50348	H	-6.16807	-2.25613	0.80169
C	1.07206	-1.93585	1.33277	H	-6.68265	-0.56961	1.03459
C	1.05877	-2.44121	-0.02488	C	-6.76082	-1.24487	-1.01614
C	2.27382	-2.01256	-0.65858	H	-7.79392	-1.59661	-0.97624
C	2.98619	-1.17788	0.25365	H	-6.76474	-0.23493	-1.43117
C	2.68794	-0.46074	2.74141	H	-6.20336	-1.90178	-1.68750
H	3.15986	0.50105	2.52417				

9. Study of the Reaction Kinetics using Complex 2 as Catalyst

The kinetics of the dehydrogenation of formic acid in toluene was investigated using complex [Cp*Ir(CO)H_2] (**2**; 0.5 mol%) as a catalyst and NEt_3 (11 mol % to FA) as a base, at temperatures ranging from 40 to 90 °C. The complete catalytic profile was analyzed using the COPASI software.[14] A simplified mechanism based on the Ir^{III} cycle represented in Fig. 4a was used as a chemical model:

$$\mathbf{CAT1} + \mathrm{FA} \longrightarrow \mathbf{CAT2} + \mathrm{H_2} \quad k_1, k_{-1} \quad \text{(eq. 1)}$$

$$\mathbf{CAT2} \longrightarrow \mathrm{CO_2} + \mathbf{CAT1} \quad k_2 \quad \text{(eq. 2)}$$

The model yielded a favorable correlation between the experimental and calculated reaction profiles using the COPASI program. The second step (eq. 2) is the rate-determining step at high formic acid concentrations. The reaction rate's independence from [HCOOH] under these conditions explains the linearity observed for the reaction profile up to approximately 80% conversion. The rate constants k_2 values, obtained by least squares regression analysis of the complete kinetic profile using the COPASI software, are presented in Table S12.

Table S12. Kinetic parameters for the dehydrogenation of formic acid in toluene (catalyst 2).[a]

Temp. (° C)	Temp. (K)	k_2 [b] (s^{-1})
90	363,15	1.203±0.015
70	343,15	0.3996±0.003
60	333,15	0.2704±0.0009
50	323,15	0.1348±0.0004
40	313,15	0.0489±0.0001

[a] HCOOH (10µL, 0.2647 mmol), NEt_3 11 mol% (4.2µL; 0.03mmol), [Cp*Ir(CO)H_2] (**2**, 0.62 mol%) as a catalyst. [b] The estimation of the parameter was conducted via the fitting of a complete kinetic profile using the COPASI software.

The activation parameters were determined from the rate constants measured at different temperatures through an analysis based on the Eyring equation:

$$\ln(k/T) = (-\Delta H^{\ddagger}/R) \times (1/T) + \ln(\kappa k_B/h) + (\Delta S^{\ddagger}/R)$$

where k is the rate constant, T is the absolute temperature, R is the ideal gas constant (8.314 $J{\cdot}K^{-1}$ mol^{-1}), k_B is the Boltzmann constant (1.380649 × 10^{-23} $J\ K^{-1}$), and h is the

Planck constant ($6.626\ 07015 \times 10^{-34}$ J s^{-1}). The transmission coefficient κ was set to the unity.

The least-squares Eyring plot of $\ln(k/T)$ versus $1/T$ showed a slope of −6699 and an intercept on the y-axis at at 12.81, with a coefficient of determination (R^2) of 0.982 (Fig. S32). This resulted in the determination of the activation parameters.

$\Delta H^{\ddagger}/R = 6699 \quad \Rightarrow \quad \Delta H^{\ddagger} = 55.7$ kJ $mol^{-1} = 13.3$ kcal mol^{-1}

$(\Delta S^{\ddagger}/R) + \ln(k_B/h) = 12.81 \quad \Rightarrow \quad \Delta S^{\ddagger} = -91.0$ J K^{-1} $mol^{-1} = -21.8$ cal K^{-1} mol^{-1}

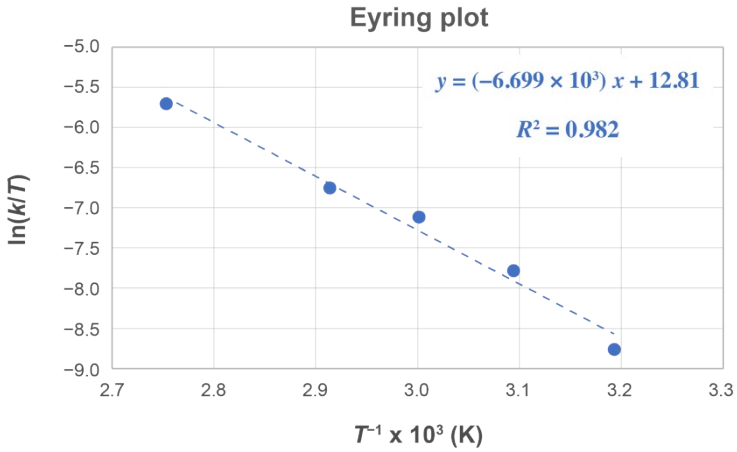

Fig. S32. Eyring plot for the dehydrogenation of formic acid in toluene using catalyst **2** (see Table S12 for conditions).

10. References

[1] R. G. Ball, W. A. G. Graham, D. M. Heinekey, J. K. Hoyono, A. D. McMaster, B. M. Mattson, S. T. Michel, *Inorg. Chem.* 1990, **29**, 2023−2025.

[2] D.M. Heinekey, D. A. Fine, T. G. P. Harper, S. T. Michel, *Can. J. Chem.* 1995*,* **73***,* 1116−1125.

[3] J. Andersen, U. Madsen, F. Björkling, X. Liang, *Synlett* 2005, 2209–2213.

[4] R. A. Evans, C. Wentrup, *J. Am. Chem. Soc.* 1996, **118**, 4009–4017.

[5] S. Sabater, H. Müller-Bunz, M. Albrecht, *Organometallics* 2016*,* **35***,* 2256−2266.

[6] M. Olivares, C. J. M. van der Ham, V. Mdluli, M. Schmidtendorf, H. Muller-Bunz, T. W. G. M. Verhoeven, M. Li, J. W. Niemantsverdriet, D. G. H. Hetterscheid, S. Bernhard, M. Albrecht, *Eur. J. Inorg. Chem.* 2020, 801–812.

[7] A. Petronilho, J. A. Woods, H. Mueller-Bunz, S. Bernhard, M. Albrecht, Iridium Complexes Containing Mesoionic C Donors: Selective C(sp^3)-H versus C(sp^2)-H Bond Activation, Reactivity Towards Acids and Bases, and Catalytic Oxidation of Silanes and Water. *Chem. Eur. J.* 2014, **20**, 15775 – 15784.

[8] G. M. Sheldrick, *Acta Crystallogr. Sect. A: Found. Crystallogr.* 2008, **64**, 112-122.

[9] L. J. Farrugia, *J. Appl. Crystallogr.* 1999, **32**, 837-838.

[10] M. J. Frisch, G. W. Trucks, H. B. Schlegel, G. E. Scuseria, M. A. Robb, J. R. Cheeseman, G. Scalmani, V. Barone, B. Mennucci, G. A. Petersson, H. Nakatsuji, M. Caricato, X. Li, H. P. Hratchian, A. F. Izmaylov, J. Bloino, G. Zheng, J. L. Sonnenberg, M. Hada, M. Ehara, K. Toyota, R. Fukuda, J. Hasegawa, M. Ishida, T. Nakajima, Y. Honda, O. Kitao, H. Nakai, T. Vreven, J. A. Montgomery, J. E. Peralta, F. Ogliaro, M. Bearpark, J. J. Heyd, E. Brothers, K. N. Kudin, V. N. Staroverov, T. Keith, R. Kobayashi, J. Normand, K. Raghavachari, A. Rendell, J. C. Burant, S. S. Iyengar, J. Tomasi, M. Cossi, N. Rega, J. M. Millam, M. Klene, J. E. Knox, J. B. Cross, V. Bakken, C. Adamo, J. Jaramillo, R. Gomperts, R. E. Stratmann, O. Yazyev, A. J. Austin, R. Cammi, C. Pomelli, J. W. Ochterski, R. L. Martin, K. Morokuma, V. G. Zakrzewski, G. A. Voth, P. Salvador, J. J. Dannenberg, S. Dapprich, A. D. Daniels, O. Farkas, J. B. Foresman, J. V. Ortiz, J. Cioslowski, D. J. Fox, *Gaussian 09*, version Revision C.01; Gaussian, Inc.: Wallingford CT, 2010.

[11] Y. Zhao, D.G. Truhlar, *Theor. Chem. Acc.* 2008, **120**, 215–241.

[12] F. Weigend, R. Ahlrichs, *Phys. Chem. Chem. Phys*. 2005, **7**, 3297–3305; F. Weigend, *Phys. Chem. Chem. Phys.* 2006, **8** 1057–1065.

[13] T. Clark, J. Chandrasekhar, G. W. Spitznagel, P. v. R. Schleyer, *J. Comp. Chem.* 1983, **4**, 294–301; M. J. Frisch, J. A. Pople, J. S. Binkley, *J. Chem. Phys.* 1984, **80**, 3265–3269.

[14] COPASI: Biochemical System Simulator, version 4.43, 2024, http://copasi.org.